AD-A114 178 ARCTEC INC COLUMBIA MD F/G 8/12
LABORATORY STUDIES OF OIL SPILL BEHAVIOR IN BROKEN ICE FIELDS.(U)
OCT 81 A P FREE, J C COX, L A SCHULTZ DTC639-80-C-80138
UNCLASSIFIED 570-C CGR/DC-1/82 NL

END
DATE FILMED
8-82
DTIC

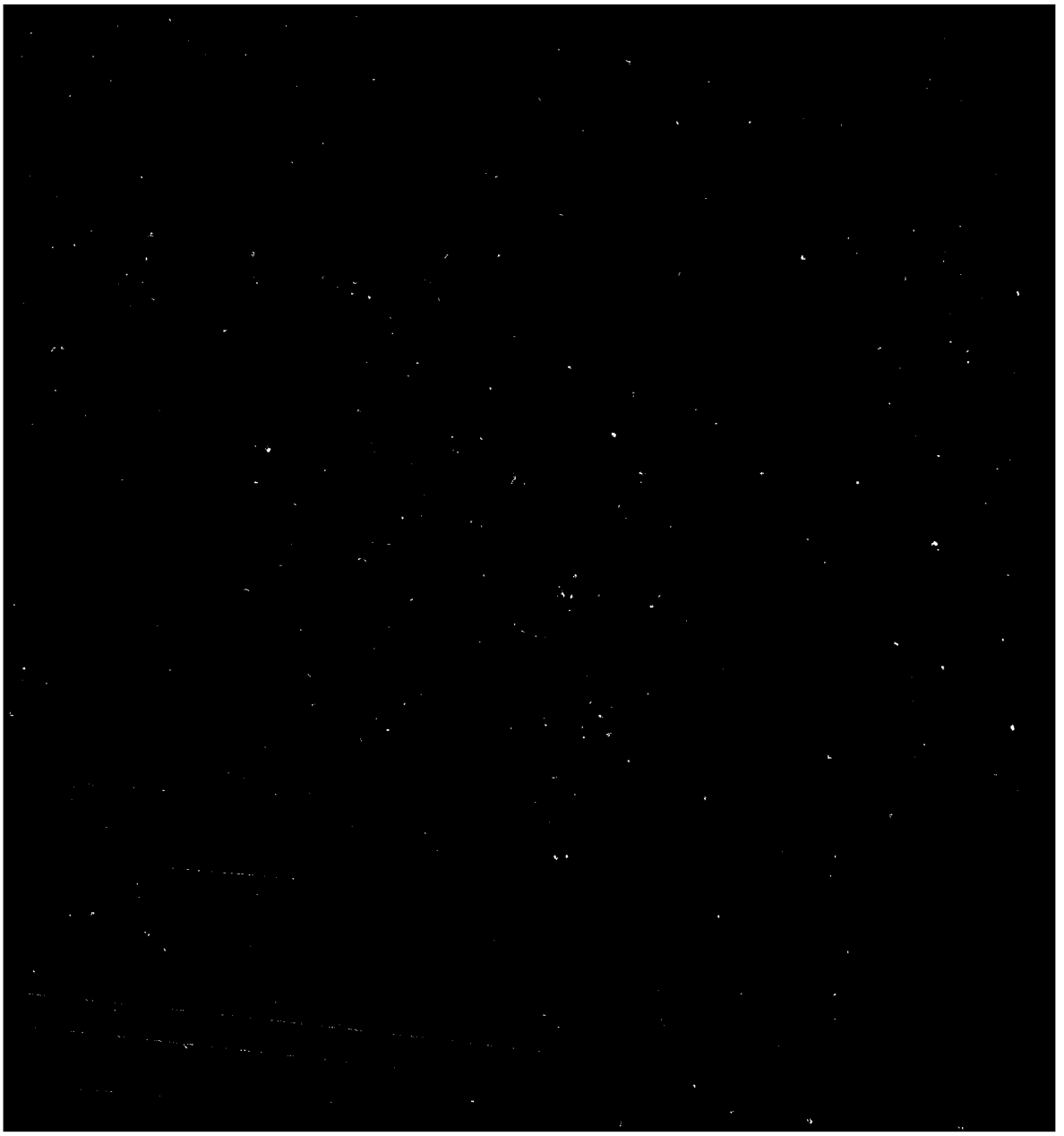

Technical Report Documentation Page

1. Report No.	2. Government Accession No.	3. Recipient's Catalog No.
CG-D-12-82	AD-A114 178	

4. Title and Subtitle	5. Report Date
Laboratory Studies of Oil Spill Behavior in Broken Ice Fields	October 1981
	6. Performing Organization Code
	8. Performing Organization Report No.
7. Author(s)	
A.P. Free, J.C. Cox, L.A. Schultz	570C
9. Performing Organization Name and Address	10. Work Unit No. (TRAIS)
ARCTEC, Incorporated 9104 Red Branch Road Columbia, MD 21045	11. Contract or Grant No. DTCG 39-80-C-80138
12. Sponsoring Agency Name and Address	13. Type of Report and Period Covered
U.S. Coast Guard Research & Development Center Avery Point Groton, CT 06340	Final Report November 1980 - November 1981
	14. Sponsoring Agency Code CGR&DC 1/82

15. Supplementary Notes

16. Abstract

This study examined the short-term behavior of oil spilled in or near a field of broken ice. The mechanics of oil seeping through the spaces between the ice blocks were examined, both on the level of a single straight gap and on the level of a random broken ice field, through experiments performed in ARCTEC, Incorporated's Ice Flume. The spreading of oil due to movement of the ice pack is discussed. The effects of the environment in the spill area, especially currents and winds, are taken into account throughout the study. The report gives information which permits the determination of the one-dimensional spread rate of oil spilled in a broken ice field, such as might be encountered in a natural lead or in a ship channel. The results are presented as a set of recommendations for use in oil spill response planning or for use by on-site response personnel in predicting the behavior of oil spilled in broken ice fields.

17. Key Words	18. Distribution Statement
Arctic Oil Spills, Oil Spills in Broken Ice, Arctic Oil Pollution, Oil Pollution, Oil Spill Response, Arctic Oil Spill Response	A

19. Security Classif. (of this report)	20. Security Classif. (of this page)	21. No. of Pages	22. Price
Unclassified	Unclassified	63	

Form DOT F 1700.7 (8-72) Reproduction of completed page authorized

METRIC CONVERSION FACTORS

Approximate Conversions to Metric Measures

Symbol	When You Know	Multiply by	To Find	Symbol
		LENGTH		
in	inches	*2.5	centimeters	cm
ft	feet	30	centimeters	cm
yd	yards	0.9	meters	m
mi	miles	1.6	kilometers	km
		AREA		
in^2	square inches	6.5	square centimeters	cm^2
ft^2	square feet	0.09	square meters	m^2
yd^2	square yards	0.8	square meters	m^2
mi^2	square miles	2.6	square kilometers	km^2
	acres	0.4	hectares	ha
		MASS (weight)		
oz	ounces	28	grams	g
lb	pounds	0.45	kilograms	kg
	short tons (2000 lb)	0.9	tonnes	t
		VOLUME		
tsp	teaspoons	5	milliliters	ml
Tbsp	tablespoons	15	milliliters	ml
fl oz	fluid ounces	30	milliliters	ml
c	cups	0.24	liters	l
pt	pints	0.47	liters	l
qt	quarts	0.95	liters	l
gal	gallons	3.8	liters	l
ft^3	cubic feet	0.03	cubic meters	m^3
yd^3	cubic yards	0.76	cubic meters	m^3
		TEMPERATURE (exact)		
°F	Fahrenheit temperature	5/9 (after subtracting 32)	Celsius temperature	°C

*1 in = 2.54 (exactly). For other exact conversions and more detailed tables, see NBS Misc. Publ. 286, Units of Weights and Measures, Price $2.25, SD Catalog No. C13.10:286.

Approximate Conversions from Metric Measures

Symbol	When You Know	Multiply by	To Find	Symbol
		LENGTH		
mm	millimeters	0.04	inches	in
cm	centimeters	0.4	inches	in
m	meters	3.3	feet	ft
m	meters	1.1	yards	yd
km	kilometers	0.6	miles	mi
		AREA		
cm^2	square centimeters	0.16	square inches	in^2
m^2	square meters	1.2	square yards	
km^2	square kilometers	0.4	square miles	
ha	hectares (10,000 m^2)	2.5	acres	
		MASS (weight)		
g	grams	0.035	ounces	oz
kg	kilograms	2.2	pounds	lb
t	tonnes (1000 kg)	1.1	short tons	
		VOLUME		
ml	milliliters	0.03	fluid ounces	fl oz
l	liters	2.1	pints	pt
l	liters	1.06	quarts	qt
l	liters	0.26	gallons	gal
m^3	cubic meters	35	cubic feet	ft^3
m^3	cubic meters	1.3	cubic yards	yd^3
		TEMPERATURE (exact)		
°C	Celsius temperature	9/5 (then add 32)	Fahrenheit temperature	°F

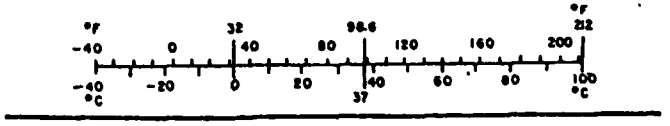

TABLE OF CONTENTS

TABLE OF CONTENTS (Continued)

LIST OF FIGURES

LIST OF FIGURES (Continued)

LIST OF TABLES

LIST OF SYMBOLS

b - ice pack characteristic dimension

c - ice pack concentration

d - dimension of an ice block

F_c - surface tension force

F_g - hydrostatic oil spreading force

g - acceleration due to gravity

K_1 K_2 K_3 K_4 K_5 K_6 - experimental constants

L - length of an ice pack

q - seepage rate of oil through a broken ice pack per unit width

t - thickness of an ice pack

v_D - velocity of the driving medium

v_i - velocity of an ice pack

v_o - velocity of oil seeping through an ice gap

w - width of a gap between two ice blocks

α - contact angle of oil with water

δ - thickness of an oil slick (reservoir)

μ_o - dynamic viscosity of oil

ρ_D - density of the driving medium

ρ_o - density of oil

ρ_w - density of water

σ_i - surface tension of oil with water

1. INTRODUCTION

The continuing energy crisis, particularly the domestic shortage of oil which increases this country's dependence on foreign oil supplies, indicates that the offshore petroleum reserves already found, and expected to be found, in arctic and subarctic ice infested regions will be developed in a timely manner. This increased activity by the petroleum industry encompassing the exploration, development, production, and transportation of oil in arctic regions will increase the potential for oil pollution in these regions.

Under the authority of the Federal Water Pollution Control Act, the U.S. Coast Guard has been charged with the responsibility of preventing and controlling the effect of oil spills in and along the coastal waters of the United States. A major portion of this area of responsibility includes the arctic and subarctic coastal waters of Alaska and other seasonally ice infested waters such as the northern rivers, the Great Lakes, and the northeastern coastal areas of the continuous 48 states. The U.S. Coast Guard has long held a leadership position in research directed towards the abatement of oil spills in cold regions.

The U.S. Coast Guard Research and Development Center has been given the specific responsibility to study oil/ice interaction phenomena and to provide guidance in defining appropriate spill response methods. The planned approach has three principle parts, consisting of a large scale, long-term oil spill trajectory model, a small scale, short-term oil spill trajectory model, and a field guide to be used by operational personnel when a spill occurs in ice infested waters.

Substantial effort by a relatively large number of researchers has been directed towards developing oil spill behavior models for open water conditions. Ice conditions or ice dynamics have generally not been included in these models. The impact of ice on oil spill behavior is so predominant that the open water spill behavior models cannot be used for ice conditions. This is true because the major forces that are applicable in the open water models no longer act directly or independently upon the oil. The forces must act through the ice or through oil/ice interaction. Previous studies performed by ARCTEC, Incorporated [2,6] examined oil interaction with smooth and rough continuous ice cover. In these cases the dominant physical phenomena were the interaction of oil with the ice and the effect of externally caused ice movement.

This report details studies made to address the behavior of oil spilled in a broken ice field, particularly on a small scale, short-term level. It is this small scale, short-term situation anlaysis that would be needed by the Coast Guard in order to mount the proper containment and cleanup efforts in the event of an oil spill in a broken ice field. The results of this research apply directly to parts two and three of the U.S. Coast Guard Research and Development Center's oil/ice study program. Sub-program areas covered by this study include the identification of the physical mechanisms of oil spreading through broken ice, determination of the environmental parameters which control oil spreading, and establishment of means of determining the extent of the spill and its spread rate. The small scale, short-term oil spill trajectory and behavior are

analyzed with direct consideration for inclusion in the forecasting spill behavior portion and the oil/ice interaction portion of the field guide.

This study consisted of two major tasks. The first task consisted of an effort to analytically describe oil spill behavior in broken ice. The results serve to suggest the possible physical mechanisms that might be involved in oil spreading through broken ice, and provide insight into the results that were obtained in the second task. The results of the analytical study are described in Section 3 of this report.

The second task consisted of experiments in ARCTEC's Ice Flume to study oil/broken ice interactions. The experimental portion of this study was made up of three individual programs. These programs were concerned with:

1. Oil flow through single gaps,

2. Oil motion through a fixed broken ice cover, and

3. Oil/ice interaction in a random unrestrained broken ice field.

The experiments were performed using a range of oil types and two ice block sizes. The effects of water currents and wind on the oil and ice motion were examined in all of the test programs. The experimental program is outlined in Section 4 of this report, and the results and observations from the tests are discussed in Section 5.

Sections 6 and 7 of the report combine the results of the two study tasks. Section 6 combines the experimental data with the analytical relationships summarized in Section 3, resulting in empirical relationships which can be used to predict the behavior of oil spilled in broken ice. Section 7 contains a description of the results of this study in a form suitable for incorporation into the field guide as a set of step by step instructions to the spill response team. By following these instructions, the spill response team can predict the probable behavior of the spilled oil with greater confidence, and implement the containment and cleanup procedures which have the greatest chances of success.

2. SUMMARY

The objective of this study was to examine the behavior of oil spilled in a broken ice field including the effects of the oil on the ice, of the ice on the oil, and of external environmental conditions such as water currents under the broken ice cover and wind forces acting on the upper surface. The study consisted of three separate, though not wholly independent, analyses:

1. Oil flow through a single narrow gap,

2. Oil spilled in a restrained field of broken ice,

3. Oil spilled in an unrestrained field of broken ice.

The project included both analytical and laboratory studies of the oil/ice interaction phenomena. The laboratory studies were conducted at low temperatures with fresh water ice in ARCTEC's glass-walled Ice Flume.

Environmental conditions were varied in the laboratory experiments, with current velocities ranging from 0 to 28 cm/s, and wind velocities ranging from 0 to 33 ft/s in model scale. These correspond to a current velocity range of 0 to 28 cm/s and a wind velocity range of 0 to 55 ft/s in full scale or field conditions. The broken ice tests were performed using two different ice block sizes, and where deemed significant, a combination of the two ice block sizes. Initial ice concentrations were varied from a low of 22% to the maximum concentration that could be obtained.

Since the properties of crude oils can vary significantly from location to location and have not yet been identified in most locations where the results of this work will be used, the tests were conducted with standard oils of known properties. Refined oils were used because the physical properties of these oils are consistent and vary less over time. The oils used were Number 2 fuel oil (diesel fuel) having low values of viscosity and density, SAE 10W oil having mid-range values of viscosity and density, and SAE 40W oil having relatively high values of viscosity and density. All of the oils were chilled to 0°C and were kept at that temperature throughout the test program.

The quantitative relationships that were developed as a result of this study are intended to characterize the short-term behavior of oil spilled in broken ice. They are intended to predict the trajectory and spread rate of such an oil spill in order to facilitate the planning of containment and cleanup measures. The results are applicable to oil spilled in broken ice in any location. The only limitation of the results is that the test conditions allowed only one-dimensional flow. The spreading phenomena for two-dimensional conditions could be significantly different. The application of these results is therefore limited to leads, ship channels, or other locations where one-dimensional flow can be assumed to exist. However, since this is the overwhelmingly common situation in the arctic, except perhaps during breakup, this is rightfully the case which should be investigated first.

The major results from this study of the behavior of oil spilled in broken ice under static conditions or in the presence of currents or winds are summarized in general terms in the following paragraphs.

2.1 Oil Containment

Oil containment, or the extent of oil containment, is a subjective quantity, based on observations. Three categories of oil containment within the broken ice field were noted during the test program. Total oil containment was judged to exist when there was no visible seepage of oil through the broken ice pack. In this case the entire oil slick was contained in and behind the broken ice field. Virtual oil containment was said to exist when small amounts of oil seeped through the broken ice pack, but the majority of the volume of spilled oil was contained behind the ice pack. The oil slick thickness contained behind the ice field was greater than the equilibrium thickness that would have existed had there been no ice. Non-containment of oil was said to exist when major portions of oil passed through the leading edge of the ice pack and into the open water beyond. Some oil may have been contained behind the ice packs at a measurable thickness, however, this was a small fraction of the spilled volume. In general, the more viscous, heavier weight oils were totally contained, and the less viscous, lighter weight oils were either virtually contained or were not contained.

2.2 Oil Flow Through a Gap

For a given oil, the oil velocity and flowrate through a single gap between ice blocks are functions of the thickness of the oil slick and the width of the ice gap. The minimum gap thickness before oil will flow through any gap is a function of the oil viscosity, surface tension, and slick thickness. Expressions were developed during this study which determined the minimum gap width required for oil to flow through the gap, and the oil velocity through gaps wider than the minimum. The flowrate through a single gap is also a function of the wind or water velocity which impose shear stresses on the oil. The effects of these external influences were incorporated in the equations for oil velocity through a single gap in the ice.

2.3 Oil Forces on Ice Blocks

When oil is released from a thick reservoir, it rapidly spreads over the water surface due to an unbalanced hydrostatic force which arises from the density difference between the oil and the water. When this moving oil encounters an ice block, this hydrostatic force is exerted upon the block and pushes the block ahead of the oil. When the oil is released behind a low concentration ice field that is restrained at its downstream end, the almost immediate result is for the oil to push all of the ice blocks towards the barrier, creating a smaller ice field of maximum concentration.

2.4 Oil Seepage Through a Field of Broken Ice

The lightweight oil (diesel fuel) was able to seep through the gaps in a packed field of broken ice. However, the gaps in the packed field of broken ice were too small for passage of the heavier weight oils which did not seep through. The

seepage rate of the diesel fuel was a function of the thickness of the oil slick, the size of the ice blocks, and the concentration of the ice pack. The seepage rate was independent of any current or wind. It appeared that the ice blocks masked the oil from these forces. An equation was developed which gives the unit width flowrate of diesel fuel through a broken ice pack.

2.5 Oil Flow Over Ice

In cases where the thickness of the oil slick was approximately equal to or greater than the thickness of the ice blocks, the oil spread over the top of the ice blocks. This occurred because the oil, especially the diesel fuel, was less dense than the ice, and therefore the ice blocks tended to "sink" in the oil. Once the oil was on top of the ice blocks, it was no longer influenced by the ice and it spread at a considerably faster open water rate. When the oil thickness decreased sufficiently, the ice blocks emerged to the surface and the oil spread rate decreased to the seepage rate through broken ice.

2.6 Oil Forces on Broken Ice Packs

When an oil slick was released behind an ice pack that was free to move, the oil exerted a hydrostatic force on the ice pack and pushed it in the same manner that it pushed the individual ice blocks. In order to move the ice pack, the oil hydrostatic force must be sufficient to overcome the resistance forces exerted by the ice pack. These resistance forces consist of the inertia force of the ice and a shear force on the ice/water interface. A minimum oil thickness exists at which the oil hydrostatic force just equals the resisting forces. At oil thicknesses less than this minimum, the ice pack will not be moved by the oil. The value of this minimum thickness is dependent upon the length of the ice field and the thickness of the ice blocks, in addition to the density of the oil. This thickness can be considerably greater than the open water equilibrium thickness of the oil.

2.7 Oil Spreading Behind a Pack of Broken Ice

A field of broken ice which is not free to move provides an effective barrier to the spread of an oil spill. The oil spreading is limited to seepage through the ice pack which normally occurs at a very slow rate, if at all. An unrestrained broken ice field, however, does not provide this effective barrier because the oil pushes the ice pack downstream. The oil slick then spreads out behind the ice pack. The ice velocity and the oil spread rate are increased further by currents and winds. Relationships were developed for determining the ice pack velocity as a function of the size of the ice field, the oil type and thickness, and the current or wind velocity. The actual oil spread rate is equal to the spread rate due to the ice pack movement plus the seepage rate into the ice field.

3. ANALYTICAL STUDY OF OIL INTERACTION WITH BROKEN ICE

Conceptually, the flow of oil through a field of broken ice can be considered as analogous to oil seeping through a series of continuous gaps between individual ice blocks. The initial phase of testing for this study examined the flow of oil through small gaps and measured the oil velocity as a function of oil slick thickness and the current or wind velocity. The second phase of testing attempted to confirm the resulting theory by measuring oil movement through fields of random broken ice which were both restrained and free to move. This section details the derivation of the oil flow relationships which fit the data obtained during the two phase test program.

3.1 Oil Flow Through a Single Ice Gap

The flow of oil in a single, fixed width gap between two ice blocks is not of itself significant, however, oil seeping through a field of broken ice encounters a series of single gaps. Examining flow through a single gap will, therefore, provide insight into the mechanisms of oil flowing through a broken ice field. This portion of the study had two objectives:

1. Determine a relationship for the minimum gap width required for oil movement through the gap (threshold of motion) as a function of oil slick properties and physical conditions, and

2. For gap widths and/or oil thicknesses greater than the threshold values, determine the oil velocity and flowrate through the gap as a function of oil properties and physical conditions.

3.1.1 Threshold of Motion Relationships

Oil tends to spread naturally over water due to a hydrostatic force which results from the difference in densities between the oil and the water. Since oil is lighter than water, it floats on the water. There is a portion of the oil layer which extends above the water surface, equal in thickness to the density difference times the oil slick thickness. Since the oil is a liquid and exhibits little shear strength, this upper portion of the oil is unrestrained and will spread over the water surface.

When two ice pieces are very close together, they are separated by a narrow gap. This gap could be so narrow as to form a capillary. Oil will leak through this gap only if the hydrostatic spreading force can overcome the surface tension force which develops at the mouth of the opening. The hydrostatic spreading force can be expressed as:

$$F_g = \int_0^{\delta} (\rho_w - \rho_o)\, g\, h\, dh = \frac{1}{2} (\rho_w - \rho_o)\, g\, \delta^2 \qquad (3.1)$$

where ρ_o and ρ_w are the densities of the oil and water respectively, g is the acceleration due to gravity, and δ is the thickness of the oil slick [3].

Capillary tension acts upon both sides of the ice gap resisting the flow of oil. The capillary force on each side of the gap is equal to [6]:

$$F = \sigma_i \, (\cos \alpha) \, \delta, \tag{3.2}$$

where σ_i is the interfacial tension between the oil and water, and α is the contact angle. Distributing this force over the width of the gap, w, yields the equation for the resisting capillary tension as:

$$F_c = \frac{2 \, \sigma_i \, (\cos \alpha) \, \delta}{w} \quad . \tag{3.3}$$

Balancing these two forces gives an expression for the minimum gap width through which oil can be expected to flow as a function of the oil slick thickness:

$$w = \frac{4 \, \sigma_i \cos \alpha}{(\rho_w - \rho_o) \, g \, \delta} \quad . \tag{3.4}$$

The minimum gap width is also a function of the oil properties. A lighter oil will have a greater hydrostatic driving force as represented by the density difference between water and oil. The lighter oil would also have a smaller value for the oil/water interfacial tension, but it will have a greater contact angle. The overall result is that a lighter oil will flow through narrower gaps than a heavier oil.

3.1.2 Oil Flow Through Gap Relationships

Once the initial surface tension effects have been overcome for oil flowing through a gap which is wider than the minimum for the oil slick thickness, the velocity and flowrate of the oil through the gap are governed by the driving force of the hydrostatic head of the oil and the resisting forces of the viscous shear stress in the oil and the friction along the sides of the gap. Any additional shear stress due to a current or a wind will also exert a driving force on the oil.

The hydrostatic oil spreading force, which is expressed in Equation (3.1), is a function of the density of the oil, ρ_o, and the thickness of the oil slick, δ. The driving force due to wind or current is a function of the density, ρ_D, and velocity, v_D of the driving medium [4]. The resisting force due to viscous shear stresses in the oil is a function of the oil viscosity, μ_o. The resisting force due to friction losses along the sides of the gap is a function of the gap width, w.

A functional relationship exists such that the velocity of the oil flowing through the gap can be expressed in terms of the four governing forces. Expressing the governing forces in terms of their independent variables allows the following functional relationship to be written:

$$\phi_1 \, (v_o, \, v_D, \, \delta, \, w, \, g, \, \mu_o, \, \rho_o, \, \rho_D) = 0 \tag{3.5}$$

Equation (3.5) can be non-dimensionalized by using v_D, ρ_D, and ω as the repeating variables as follows:

$$\phi_2 \left[\frac{v_o}{v_D}, \frac{\delta}{\omega}, \frac{\rho_D \omega v_D}{\mu_o}, \frac{v_D^2}{g\omega}, \frac{\rho_o}{\rho_D}\right] = 0 \ . \tag{3.6}$$

Since $\rho_D \omega v_D/\mu_o$ has the form of a Reynolds Number, and $v_D^2/g\omega$ has the form of a Froude Number, Equation (3.6) may be rewritten to read:

$$\phi_3 \left[\frac{v_o}{v_D}, \frac{\delta}{\omega}, \frac{\rho_o}{\rho_D}, Re, Fr^2\right] = 0 \ . \tag{3.7}$$

Equation (3.7) states that the oil velocity through a gap relative to the water or wind velocity helping to drive it through the gap can be expressed as a function of the oil thickness to the gap width ratio, the ratio of the density of the oil to that of the driving medium, a Reynolds Number of the oil/water or oil/air interface, and a Froude Number for water moving through the gap.

The Reynolds Number expresses the ratio of the inertial driving forces to the viscous resisting forces in the oil. The Froude Number expresses the ratio of the inertial driving forces to the resisting forces in the gap. The ratio of the oil to driving fluid densities reflects the shear stress exerted on a given oil by the driving fluid. Therefore, for a given slick thickness to gap width ratio, one would expect the following relationship to hold:

$$\frac{v_o}{v_D} = K_1 \left(\frac{Re}{Fr^2}\right) \left(\frac{\rho_o}{\rho_D}\right) + K_2 \tag{3.8}$$

where K_1 is a function dependent upon the slick thickness to gap width ratio and the oil properties, and K_2 is a function dependent upon the oil properties. A more detailed derivation of these equations is given in Appendix C.

3.2 Oil Spreading in the Presence of a Field of Broken Ice

Oil spreading in a random broken ice pack, such as could be expected in certain field conditions, has two components. The oil will seep through the gaps in the broken ice pack, and the oil will spread behind the ice pack as the pack moves due to current, wind, or forces exerted by the oil. If the ice pack is restrained, the oil spreading will consist only of seepage through the gaps.

This portion of the study has the following objectives:

1. Determine a relationship that expresses the effects that a broken ice cover has on the spreading of oil. This involves the derivation of a relationship for the seepage rate of oil through a random broken ice pack. Included is an analysis of the theory presented in the previous section to determine if the relationship developed for flow through a single gap correctly describes motion through a broken ice field.

2. Determine a relationship for the spreading of oil behind an unrestrained broken ice pack due to the movement of the ice.

3.2.1 Oil Seepage Through a Field of Broken Ice

The seepage of oil through an ice pack should follow the expression derived for the velocity of oil through a single gap, which was presented in Section 3.1.2. However, the gap width, which was assumed to be a known constant value in the single gap case, is variable throughout the ice field, and is not necessarily known. In addition, the channel formed by the connecting gaps between the ice blocks meanders throughout the field, causing the oil to take a torturous wandering path between the ice blocks. This obviously greatly increases the friction losses between the oil and the ice. For these reasons, it appears that application of Equation (3.8) to determine the oil seepage velocity through the ice pack is impossible.

The gap width between the ice particles in a random broken ice pack is a function of the size of the ice blocks and the concentration of the ice pack. If a rectangular packing arrangement is assumed, the concentration (c) of the broken ice pack can be expressed as:

$$c = \frac{A_i}{A} = \frac{d^2}{(d + b)^2} , \tag{3.9}$$

where d is the size of an individual ice block and b is the gap between each ice block. This gap width, b, is a function of the size of the ice blocks and the ice pack concentration. It can be considered to be a characteristic field dimension and can be used to serve as a parameter similar to the gap width for determining the oil seepage rate through the ice pack. Rearranging Equation (3.9)gives the expression for this theoretical gap width as:

$$b = d \left(\frac{1}{\sqrt{c}} - 1\right) \tag{3.10}$$

where d is the size of an individual ice block. In cases where more than one ice block size exists, up to m different block sizes, d is obtained as follows:

$$d = n_1 d_1 + n_2 d_2 + \ldots + n_n d_m \tag{3.11}$$

where n is the fraction of ice blocks of size d.

For a given type of oil, the oil flowrate through a broken ice field per unit width, q, is a function of the thickness of the oil slick, δ, and the characteristic dimension of the ice field, b, just defined. Expressed in non-dimensional form, this relationship can be stated as:

$$\frac{q^2}{g\, b^3} = K_3 \left(\frac{\delta}{b}\right)^{K_4} \tag{3.12}$$

where K_3 and K_4 are constants.

Although the oil slick thickness in most cases is large, in the same range of thickness as the ice thickness, the oil layer seeping through the ice field is very thin, much less than the thickness of the ice. One can consider

the ice blocks to be large scale roughness elements in the oil flow channel. As water flows under the ice pack a boundary layer between the current and the underside of the ice pack is formed. The water velocity at the top of this boundary layer, where the oil is flowing, is negligible. It therefore appears that Equation (3.12) will apply whether or not a current exists. The accuracy of this assumption will be determined during the test program as will the effects of wind.

3.2.2 Oil Spreading with a Moving Broken Ice Field

An oil slick spilled behind an unrestrained broken ice field will spread at the rate at which the ice field moves plus the rate at which the oil seeps between the ice blocks. The previous section examined the rate of oil seepage through a broken ice field. This section examines the rate of movement of a broken ice field due to oil, current, and wind forces.

There are two driving forces which can act together to move an unrestrained ice field. These forces are the shear force exerted on the ice either by current or wind, and the hydrostatic force exerted on the ice by the oil. Two forces will act to resist the motion of the ice pack. These forces are the inertia or weight of the ice blocks, and the form drag around the leading edge of the ice field as it pushes through the water.

From Equation (3.1) it can be seen that the hydrostatic driving force due to the oil varies with the square of the oil slick thickness, δ, for a given type of oil. The inertial force of the ice is a function of the amount of ice in the ice field. This can be expressed in terms of the length of the ice field, L, for a unit width. Assuming that the surface roughness of the ice is a constant, the form drag on the leading edge of the ice pack can be expressed as a function of the ice thickness, t, per unit width. From the above relationships an expression can be written for the velocity of an ice pack in the presence of an oil slick for a given water or wind velocity as follows:

$$v_i = K_5 \left(\frac{\delta^2}{tL}\right) + K_6 \tag{3.13}$$

where K_5 is a constant dependent upon the properties of the spilled oil and K_6 is a function of the current velocity and the oil properties.

The relationship expressed by Equation (3.11) becomes inaccurate at small values of δ^2/tL. At these values, the hydrostatic force of the oil is not large enough to overcome the resistance forces. As this ratio decreases, the ice pack velocity gradually decreases to the velocity that the ice pack would have under oil free conditions. This will occur as the oil slick becomes thin due to the spreading of the oil behind the moving ice pack.

4. EXPERIMENTAL PROGRAM

The experimental program was performed in ARCTEC's glass-walled Ice Flume. The test program was divided into three parts. The initial set of tests examined the flow of oil through a single gap between ice blocks. The second set of tests examined the dynamics of packs of broken ice under the influence of current or wind, without oil. The third set of tests examined the interaction of oil with broken ice packs, which were both restrained and free to move. The influence of wind or currents on the oil and ice dynamics were tested. The results of these tests were used to determine the validity of the analytical studies which were presented in Section 3. This section covers the general details of the formulation of the test program, and the procedure used in each of the tests.

4.1 Selection of Test Oils

The types of oils that could be spilled in an ice infested area could be numerous. The most probable types of oil that could be spilled in an ice region are diesel oil from a ship's fuel tanks or crude oil from either a tanker or a well. However, in the case of crude oil, the properties of the spilled oil cannot be predicted. Therefore, a group of refined oils with constant, known properties were used in this test program, selected so as to span the range of oil properties that might be encountered in the case of an oil spill in ice infested waters.

ASTM Committee F-20 recommends testing with three types of oils:

1. A light oil with viscosity between 3 and 10 centistokes at 60°F, and specific gravity between 0.83 and 0.88,

2. A medium oil with viscosity between 100 and 300 centistokes at 60°F, and specific gravity between 0.90 and 0.94, and

3. A heavy oil with viscosity between 500 and 2,000 centistokes at 60°F, and specific gravity between 0.94 and 0.97.

Refined oils are desirable for laboratory testing because their properties do not tend to vary with time. Taking these factors into account along with the availability of small quantities (100 gal) of these oils, three oils were selected for testing: diesel fuel oil (Number 2 fuel oil), SAE 10W oil, and SAE 40W oil. The significant properties of these oils are given in Table 4.1.

TABLE 4.1 TEST OIL PROPERTIES

OIL	DENSITY (g/cm^3)	VISCOSITY (poise)	POUR POINT (°C)	INTERFACIAL TENSION (g/sec)	CONTACT ANGLE (degrees)
Number 2	0.857	0.07	-18	18.0	20
SAE 10W	0.880	3.54	-29	23.2	30
SAE 40W	0.901	37.5	-13	26.9	40

4.2 Scaling Considerations

When testing with two different types of fluids, and particularly when trying to use prototype fluids, scaling considerations can become insurmountable problems. Therefore, the entire test program was run at full scale. This is because the properties of the water and the oils are full-scale by nature and cannot be scaled down. In order to obtain valid results it becomes extremely important to match the pertinent velocities or forces between field and laboratory conditions. Since it is virtually impossible to match water or wind velocity profiles in a flume or wind tunnel to the actual field conditions, it is necessary to examine the basic driving mechanisms which these conditions will exert upon the oil and ice. The shear forces which the wind or current exerts upon the oil and ice must be equal in both the prototype and the model in order to satisfy scaling considerations.

Cox, et al [2] examined the water velocity profiles under a solid ice cover in ARCTEC's Ice Flume and compared these results against those measured in the field. They concluded, by matching the shear stresses created on the underside of the ice, that the current velocities were full scale and could be matched to field conditions directly.

In order to match the shear stress exerted by the wind under field conditions to that created in the wind tunnel during testing, the friction factor between ice and air must be considered. The shear stress exerted on a surface by a flowing fluid is equal to:

$$\tau_s = \alpha \, \rho_f \, v_f^2 \ , \tag{4.1}$$

where α is a roughness coefficient, ρ_f is the density of the fluid, and v_f is the velocity of the fluid. Based on an air speed of 20 ft/s the friction factor for the ice blocks in the wind tunnel was estimated to be 0.046. The roughness coefficient can be related to the friction factor by:

$$\alpha = \frac{f}{8} \ . \tag{4.2}$$

The shear stress exerted upon the ice blocks in the wind tunnel is equal to:

$$\tau_{sMODEL} = \frac{f_{MODEL}}{8} \, \rho_{AIR} \, v_{MODEL}^2 \ . \tag{4.3}$$

Field measurements reveal that the roughness coefficient, C_{10}, based on a wind speed measured at a height of 10 meters, ranges from 0.0010 to 0.0023 [1]. The shear stress exerted upon the ice in the field is equal to:

$$\tau_{sFIELD} = C_{10} \, \rho_{AIR} \, v_{FIELD}^2 \ . \tag{4.4}$$

Equating the shear stresses in Equations 4.3 and 4.4 gives:

$$\frac{f_{MODEL}}{8} \, v_{MODEL}^2 = C_{10} \, v_{FIELD}^2 \ . \tag{4.5}$$

The scale factor between the laboratory wind tunnel and the field condition is then equal to:

$$\frac{v_{FIELD}}{v_{MODEL}} = \left(\frac{\tau_{MODEL}}{8\, C_{10}} \right)^{1/2} . \qquad (4.6)$$

Assuming a value for C_{10} of 0.002, a laboratory wind speed of 20 ft/s is roughly comparable to a field wind speed of 34 ft/s. The wind tunnel scale factor is then 1:1.7.

4.3 Oil Properties Testing

Before the start of tests each day the physical properties of the oils to be used in testing that day were measured and recorded. These daily measurements were necessary to insure that no property variations took place in the oils due to aging, temperature changes, or non-uniformity of the oil samples. The oils were stored in ARCTEC's Cold Room, therefore, the oil temperature was always in the range of -2° to 0°C. Oil temperature was measured using an ASTM approved laboratory thermometer, accurate to 0.1°C over a range of -20°C to 10°C.

The oil properties measured included specific gravity or density, viscosity, and surface tension. Oil density was measured with two specific gravity scale hydrometers which meet ASTM Specification E100-66. Oil viscosity was measured with a Brookfield Model LVF Synchrolectric Viscometer, which is described in Appendix A, using the procedure outlined by ASTM Specification D2983-72. Interfacial tension measurements were made with a Model 20 Fisher Surface Tensiometer, which is also described in Appendix A, using the procedures outlined in ASTM Specification B-971 and D-1331.

4.4 Single Gap Tests

The first phase oil flow tests were performed to determine the rate at which oil would flow through a single, straight ice gap of known width, both with and without external forces applied in terms of a driving current or wind. Water velocities were varied from 0 to 28 cm/s, and wind tunnel velocities were varied from 0 to 2,000 ft/min.

Two ice blocks were grown in the flume. A gap of known thickness was then cut between the two blocks. A thick oil reservoir was created upstream of the ice blocks. The current or wind was turned on and the oil was released from the reservoir. Oil velocity was measured by timing small tracers on the oil surface as they traveled a known distance. The thickness of the oil reservoir was measured using a ruler at specific time intervals during the test. Oil flowrate was calculated from the change in thickness (volume) of the reservoir over time. Movies and still photographs were taken throughout the tests. The cleanup procedures used after the completion of the tests are outlined in Appendix B.

All three oils were tested in this phase. Four water velocities and four wind velocities were used to drive the oil through the gap. The gap widths tested ranged from the minimum gap that would allow oil flow, to gaps so wide that the ice had no influence on the flow of the oil, and open water conditions existed.

4.5 Oil-Free Broken Ice Tests

The first portion of the broken ice cover testing consisted of experiments run in the Ice Flume using the ice blocks but no oil. This portion of the testing provided background information against which the results of the oil/ice interaction testing could be compared. From this information, the changes in the dynamics of the ice that were caused by the oil could be identified.

In each test the ice blocks were arranged in a tightly packed, random field, with barriers both upstream and downstream. The current or wind was turned on and the barriers were removed. The ice flowed downstream in the flume under the influence of the current or the wind. The velocity of the front of the ice field was measured by moving the flume carriage, described in Appendix A, downstream with the ice front. The velocities of intermediate locations and the back of the ice field were measured by following specially dyed ice blocks downstream, and recording their distance downstream over time. The initial and final field lengths were measured, along with the amount of ice placed in the flume, to determine the ice concentration and the extent to which the ice field spread out. Movies and still photographs were taken of the initial and final conditions, and throughout the tests.

Both ice block sizes, 3.25 inches and 6.5 inches, were tested individually, and a combination field consisting of both block sizes was also tested. Four water velocities were tested, ranging from 0 to 27 cm/s. Four wind velocities were tested, ranging from 0 to 2,000 ft/m in model scale.

4.6 Oil Spreading Through a Restrained Broken Ice Field

In order to determine the flowrate at which oil will spread through the gaps in a broken ice field, tests were performed in which oil was introduced at the back of a field of broken ice that was restrained by a permeable barrier. This barrier consisted of a screen with very large mesh which did not allow passage of the ice blocks, but which gave no resistance to the passage of oil or water. The oil was supplied from an oil reservoir formed behind the ice field at a thickness approximately equal to that of the ice.

Ice blocks were placed behind the permeable barrier in a random ice field. The concentration of the blocks placed in the field ranged from 23% to 80%. A baffle was placed at the back of the ice field behind which the oil reservoir was formed. If current or wind were to be used, they would be turned on. Tests were also performed to measure the static spreading of the oil without current or wind. The baffle between the ice and the oil was then removed. Measurements were taken over time of the thickness of the oil slick. The time required for the oil to seep through the ice field was recorded, if this occurred. If the oil did not seep through the field, the time to establish an equilibrium condition, and the depth of penetration into the ice field were recorded. The final ice field length was measured to give the final ice concentration. Movies and still photographs were taken before, during, and after completion of the test.

Both 3.25 inch and 6.5 inch ice blocks were used in this test. Tests were performed with no wind or current, with wind speeds ranging from 600 to 2,000 ft/min, and with current speeds ranging from 6 to 22 cm/s. All three types of oil were tested.

4.7 Oil Spreading Through an Unrestrained Broken Ice Field

The final phase of laboratory testing consisted of measuring the spread of oil spilled in an unrestrained broken ice field. The tests were performed under static conditions or under the influence of current or wind.

A broken ice field approximately ten feet long was formed behind a barrier in the ice flume. The ice was randomly arranged at high concentration. The initial ice concentration was recorded. Two additional barriers were placed in the ice field, one at the back of the field and one approximately one third of the way from the back of the field. An oil reservoir was formed in this approximately 3.5 foot long section. The oil thickness was approximately equal to that of the ice. If required, the wind or current was turned on. The three barriers were removed and the oil and ice flowed downstream. The carriage pointer was moved with the front of the ice to record the ice front velocity as outlined in Appendix A. The location of the oil front and the back of the ice field were recorded at certain intervals to determine the velocity of the oil, the penetration of the oil into the ice field, and the concentration of the ice field. Movies and still photographs were taken before, during, and after the tests.

Both ice block sizes were used in the unrestrained ice field tests, both individually and in combination. The wind velocities tested ranged from 0 to 2,000 ft/min. The water velocities tested ranged from 0 to 23 cm/s. The diesel fuel and the SAE 10W oil were used in these tests. The SAE 40W oil was not used because it acts very similar to the SAE 10W oil. This allowed more in depth testing of the two oils which were used.

5. RESULTS OF THE EXPERIMENTAL PROGRAM

This section of the report provides a general discussion of the observations made during the experimental program and a general overview of the experimental data that was obtained. Detailed analysis of the data and the application of the data to the equations discussed in Section 3, are left to the following section.

5.1 Oil Containment

Oil containment in a broken ice field can be classified under one of three categories. All of these containment categories were observed during both the single gap test program and the broken ice field test program. The three oil spill containment categories are total containment, virtual containment, and non-containment.

Total oil containment occurs most often with the heavier, more viscous oils. For this case, the oil does not seep from the thick oil slick through the broken ice field, rather all of the spilled oil remains trapped in the initial oil slick and in the gaps between the ice blocks adjacent to the slick. The thickness of the oil slick contained behind the ice field was of the order of several centimeters, which is much greater than the equilibrium thickness that the oil would have spread to in open water. Total containment generally occurred with the SAE 40W oil, and sometimes occurred with the SAE 10W oil. Total containment occurs when an oil slick is thinner than the thickness required by Equation (3.4) for the given oil and ice gaps. There is insufficient hydrostatic force to drive the oil through the gaps between the ice blocks.

Virtual containment is rather a subjective term, however, it can best be defined as existing when the major portion of the oil spill volume is contained in the gaps in the ice field and/or the oil reservoir, and only a small quantity of oil is seeping through the ice field to open water. Virtual containment may be difficult to identify because it can be easy to over-estimate the oil flowrate based on visual observations of the oil seeping through the ice field. However, by measuring the amount of oil lost from the oil reservoir, it can be seen that in most cases the oil flowrate through the broken ice field is actually quite small. As with total containment, the thickness of the upstream oil reservoir is considerably greater with virtual containment than the slick thickness would be in ice-free equilibrium conditions. Virtual containment was observed in most of the tests with the SAE 10W oil and with the diesel fuel. Analytically, virtual containment indicates that the gaps in the ice field were only slightly larger than the threshold of motion gap widths predicted by Equation (3.3) for the particular oil and reservoir thickness.

Non-containment occurs when the ice gives little or no resistance to the flow of the oil. The oil will spread at a rate nearly equal to its open water spread rate. The thickness of the oil slick approaches the open water equilibrium slick thickness. Non-containment was only observed with the light, low viscosity diesel fuel oil. The initial ice concentration in most of the cases was so small that there were large gaps between the ice blocks which the oil could flow

through. In the remainder of these cases the oil reservoir thickness was so large that the oil surface was higher than that of the ice blocks. The oil flowed over the top of the ice field, submerging the ice blocks. As the oil thickness decreased, however, the ice blocks resurfaced and formed a barrier providing virtual containment to the remaining oil in the reservoir.

Total, virtual, and non-containment were observed in the single gap tests as well as the broken ice field tests. For each oil there was a minimum gap width through which the oil would initially start to flow. Any gap smaller than this minimum gap would provide total oil containment. At larger gaps, up to the range of several inches with the heavier oils, virtual containment would exist, with most of the oil being trapped in the reservoir behind the ice. When the gaps became very large, the oil would no longer be contained and would spread at a rate nearly equal to that for open water conditions. Gaps of six inches or greater were normally required for this to occur with the heavier oils. Light oils have much smaller minimum gap requirements. Extremely narrow gaps are required to totally contain diesel fuel. The diesel fuel would flow at open water rates with gaps of only two or three inches.

5.2 Oil Forces on Ice Blocks

Because of the fact that the oil is less dense than either water or ice, oil exerts hydrostatic forces on the ice blocks. These forces act in both the horizontal and vertical directions and are the significant driving forces behind the seepage of oil through a broken ice field.

The horizontal hydrostatic force is the driving force that causes oil to spread over open water. Because the oil floats on the water, its surface is higher than the water surface as is shown in Figure 5.1. An unbalanced hydrostatic pressure exists in that portion of the oil which is above the water surface. This force will be exerted on any ice block encountered by the spreading oil slick, which then pushes the block in the direction of oil spreading. The result of this force was to always keep an ice field compacted to its maximum concentration. In the restrained ice field tests, where the initial ice field concentrations were as low as 23%, the ice field was compacted to the maximum concentrations of 80 to 90% almost immediately upon release of the oil from the reservoir. For this reason, the ice pack almost always provided total or virtual containment of the oil independent of the initial ice concentration. This can be clearly seen in Figures 5.2 and 5.3. Figure 5.2 shows an initially loosely arranged ice field prior to the release of the SAE 40W oil from the reservoir. Figure 5.3 shows the tightly packed ice field at equilibrium after the SAE 40W oil had been released. Also note that the oil had come to rest without fully penetrating the ice pack. The oil is totally contained by the broken ice field.

In the tests where the ice field was free to move, the oil significantly reduced the spreading of the ice pack, maintaining it at a high concentration. The oil induced a velocity in the ice pack which was usually greater than the water velocity.

The unrestrained ice pack resisted the horizontal motion which is initiated due to the force of the oil. This resistance was the result of internal friction in the ice pack, shear along the sides of the flume, and shear at the ice/water interface. The oil reservoir needed to have a thickness in the range of 1 to 2 cm to overcome this resistance. The actual oil thickness

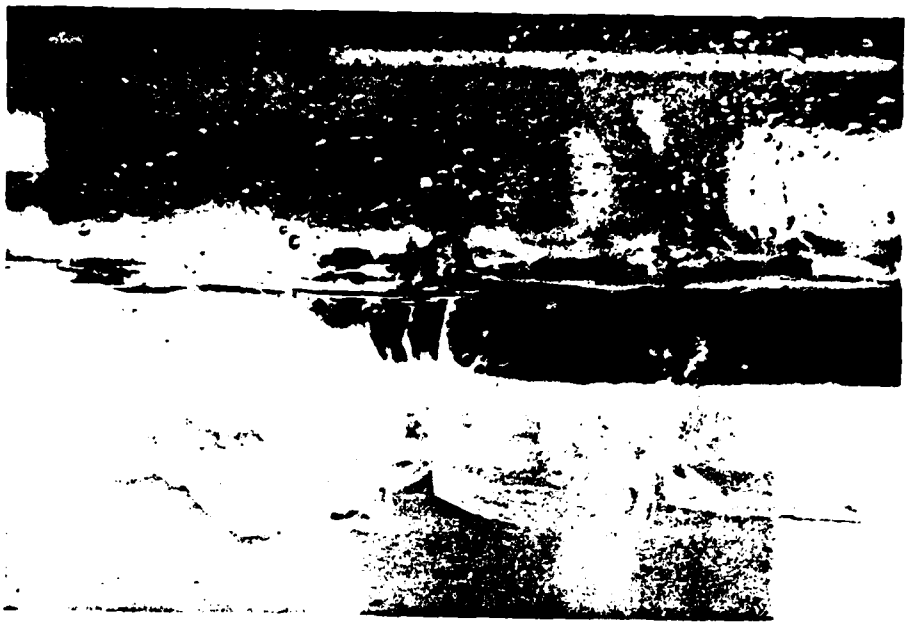

FIGURE 5.1. Photo of Oil Contained in a Broken Ice Field in ARCTEC's Ice Flume Showing Surface Variations Between the Oil, Ice, and Water.

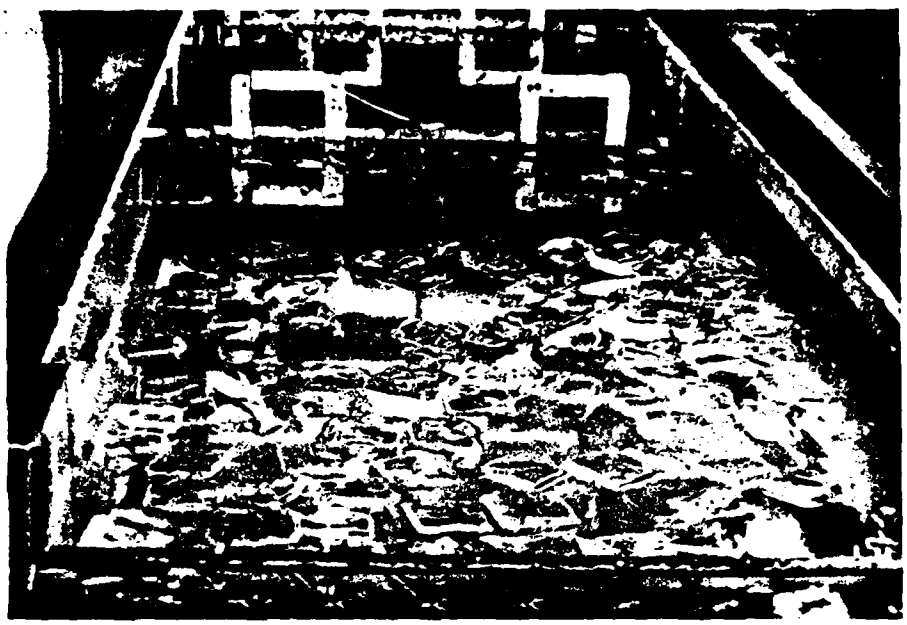

FIGURE 5.2. Photo of the Initial Condition of a Loosely Arranged Ice Field Prior to the Release of SAE 40W Oil From the Reservoir

FIGURE 5.3. Photo of the Ice Field of Figure 5.2 at Equilibrium After the Release of the SAE 40W Oil Which Compacted the Ice Field

that is required to overcome this resistance is a function of the oil density, the weight of the ice, and the draft of the ice blocks. At oil thicknesses below this minimum, the effect of the oil on the ice pack will be small, and the ice pack velocity will decrease to the oil-free ice pack velocity.

The vertical hydrostatic force is exerted by the oil on the ice because the oil is less dense than the ice. When oil is placed in a reservoir that is approximately the same thickness as the ice blocks, it will have a surface elevation that is higher than the blocks as is shown in Figure 5.1. When the oil is released it will flow over the top of the blocks, approximating open water conditions. This initial non-containment situation is temporary, however, because the oil thickness will decrease as the oil surface area increases, until the surface elevation of the oil is less than that of the ice blocks. The oil must then flow through the gaps in the ice field. This normally results in virtual containment of the remaining oil within and behind the ice field.

5.3 Ice Field Concentration

The concentration of a broken ice pack as the term is used throughout this report is the surface concentration. This concentration is defined as the percentage of surface area of an ice field which is covered with ice. To determine the concentration, the dimensions of an ice field comprised of a known number of ice blocks of known size were measured. The concentration was calculated from the following equation:

$$c = \frac{n\ d^2}{W\ L} \tag{5.1}$$

where n is the number of ice blocks, d is the dimension of the cubic ice blocks, W is the width, and L is the length of the ice field.

Under the influence of the oil, the ice field is compressed to a maximum concentration. Because of the randomness of ice block arrangement, this maximum concentration does not approach the theoretical maximum value of 1.0. The maximum concentrations measured during the test program were 0.80 to 0.85 for the small ice blocks, and 0.85 to 0.90 for the large ice blocks. The maximum concentration of a field of small ice blocks is less than that for a field of large ice blocks because the smaller block size allows for a greater randomness and a less regular packing arrangement.

5.4 Current Effects on Oil Movement

Cox, et al [2] examined the trapping of oil both upstream and downstream of large roughness elements under ice covers. They determined that oil can be trapped and insulated from the effects of an underside current in a vortex region just downstream of a large roughness element. The size of this entrapment is a function of the water velocity. Considering the broken ice field to be a number of large roughness elements grouped very close together, one would expect that an oil layer, somewhat thinner than the ice block thickness could be trapped in the broken ice pack and not have a shear force exerted on it by an underside current. The maximum thickness of this hypothetical layer would be a function of the water velocity.

The test program proved the above assumption to be correct. The velocity of the oil spreading through the broken ice field was not increased by the water velocity. The seepage rate of the oil through an ice field with no current was measured to be the same as that which occurred with a high water velocity, for constant oil thickness and ice conditions. The ice blocks insulated the thin oil layer from the effects of the water velocity.

5.5 Wind Effects on Oil Movement

The mechanics of wind exerting a force on the oil or the ice blocks are the same as those for a current. Both exert a turbulent shear stress on the oil or ice, pushing them in the direction of the wind or current. During the test program, the same type of phenomena were observed to occur with both wind and currents, however, the oil and ice velocities due to the wind were much less than those measured due to the current. This indicates that although the wind velocities were higher than the water velocities, the shear forces exerted by the wind on the oil and ice were much less than those exerted by the water. Because of this, wind tests were omitted where they would yield no additional useful information. This allowed more attention to be focused on the most significant problems.

6. ANALYSIS OF TEST RESULTS AND EMPIRICAL RELATIONSHIPS

This section combines the equations which were derived in Section 3 with the data obtained during the test program. The validity of the equations to adequately model what was observed in the lab is discussed. The experimental constants in the equations are determined, and the equations are generalized to fit as many situations as possible.

6.1 Threshold of Motion

As was discussed in Section 3, the driving force which causes oil to flow through a gap between two ice blocks is the hydrostatic force arising from the difference in density between the oil and the water. The resisting force to the flow of oil between small gaps is the surface tension of the oil at the entrance of the gap. For any given gap width there exists an oil slick thickness at which these two forces balance. This thickness can be considered to be the threshold of motion thickness for this gap. A thinner slick will not have sufficient driving force to allow oil to flow through the gap. A thicker slick will have oil flowing through the gap.

Equation 3.4 states the theoretical relationship between oil reservoir thickness and single ice gap width at the threshold of motion:

$$w = \frac{4\ \sigma_i \cos\ \alpha_i}{(\rho_w - \rho_o)\ g\ \delta} \quad . \tag{3.4}$$

Plots of Equation 3.4 for the three test oils are given in Figure 6.1. The measured oil properties used in Equation 3.4 are given in Table 4.1. Also plotted on Figure 6.1 are the results of the threshold of motion experiments. The experimental data and the theoretical curves are not in close agreement, however, they are of the same order of magnitude. The results clearly indicate that an oil slick thickness in the range of several centimeters is required for oil to flow through the rather narrow gaps in a compacted broken ice field.

6.2 Single Gap Test Results

Shown on Figures 6.2, 6.3, 6.4, and 6.5 are plots of the velocity of SAE 10W oil through a single ice gap versus oil slick thickness. A series of single gap widths are plotted on each figure, and the current velocity is varied between the figures. Plots drawn for the other oils tested or those for the wind tunnel tests have the same form as these figures.

Clearly, although plots such as those shown in Figures 6.2, 6.3, 6.4, and 6.5 are useful, a more general form is required. Recall from the theoretical analysis in Section 3 that a non-dimensional equation was written which related the velocity of the oil to the current velocity, the gap width and the relative density of the oil to the density of the driving fluid for a given oil thickness to gap width ratio as follows:

$$\frac{v_o}{v_D} = K_1 \left(\frac{Re}{Fr^2}\right)\left(\frac{\rho_o}{\rho_D}\right) + K_2 \quad . \tag{3.8}$$

FIGURE 6.1
THRESHOLD OF MOTION
RESERVOIR THICKNESS VS SINGLE GAP WIDTH

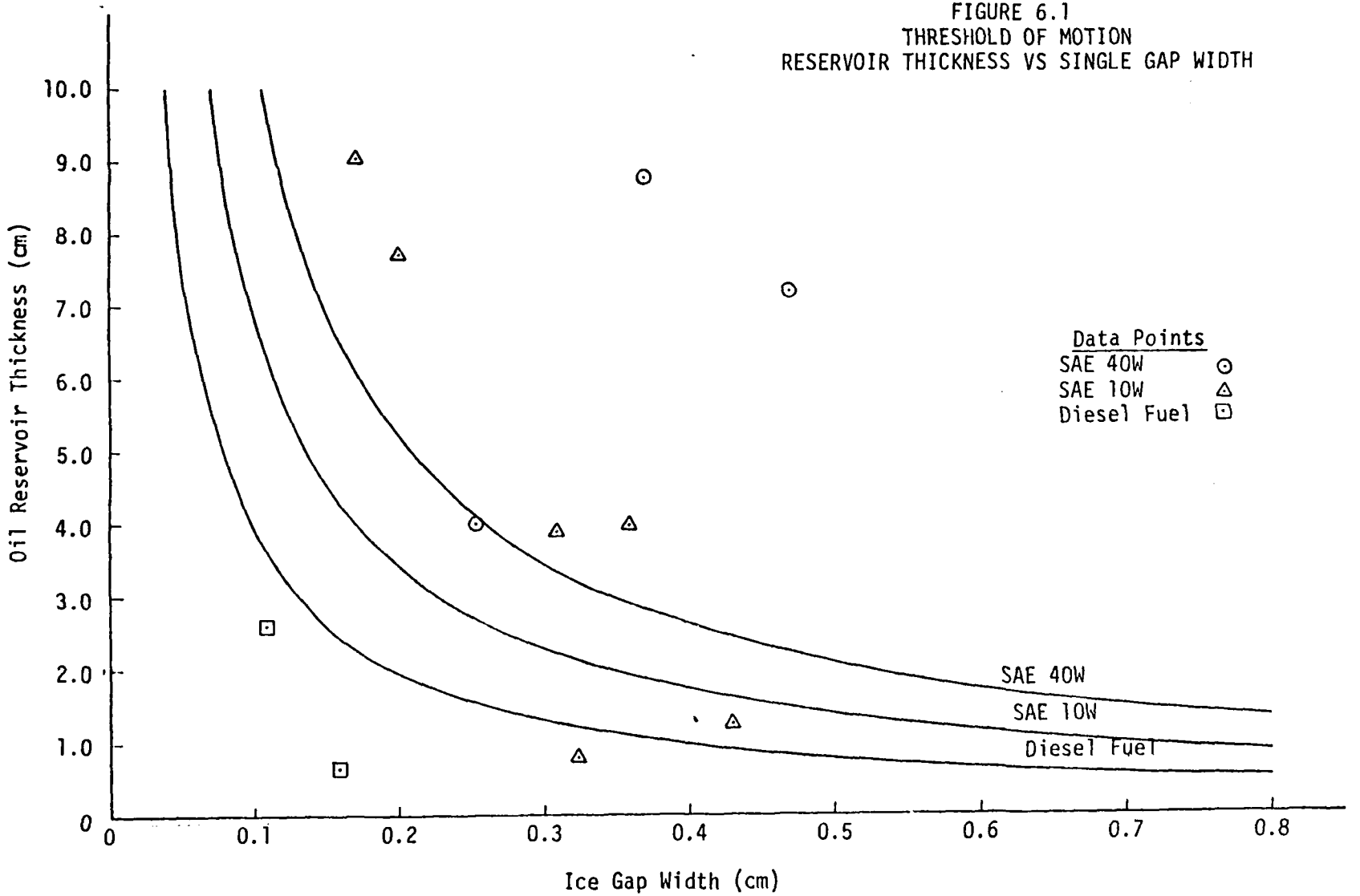

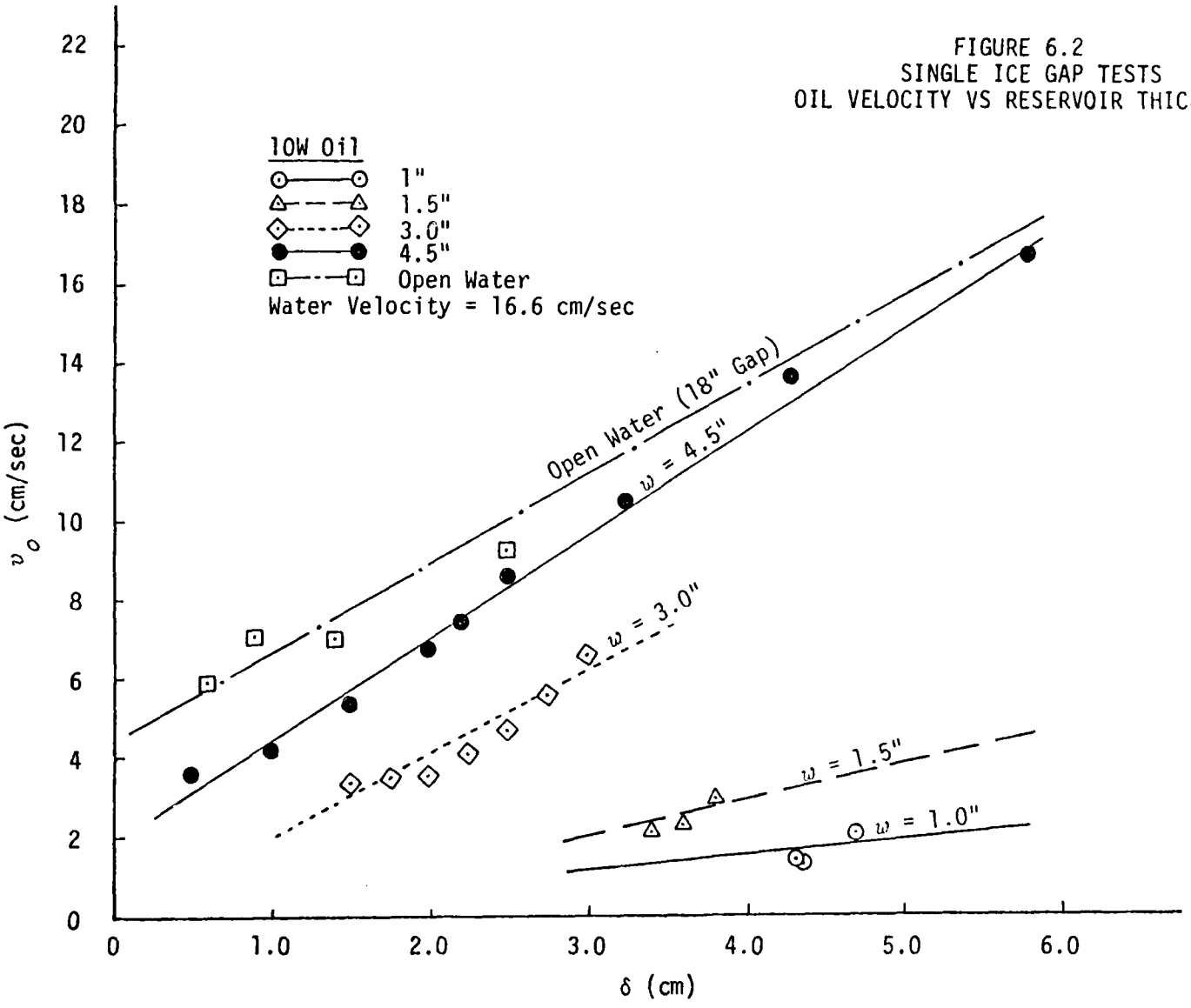

FIGURE 6.2
SINGLE ICE GAP TESTS
OIL VELOCITY VS RESERVOIR THICKNESS

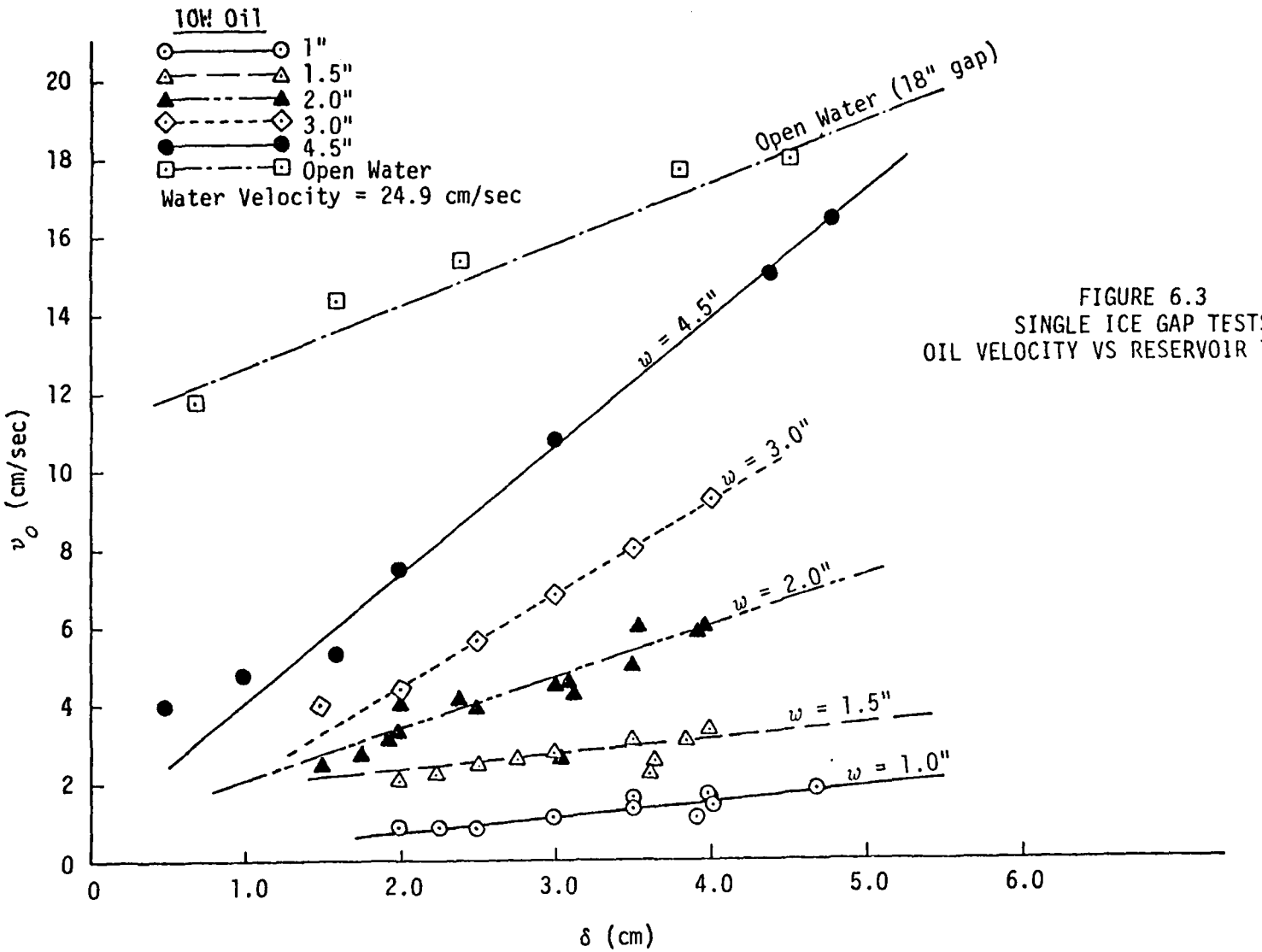

FIGURE 6.3
SINGLE ICE GAP TESTS
OIL VELOCITY VS RESERVOIR THICKNESS

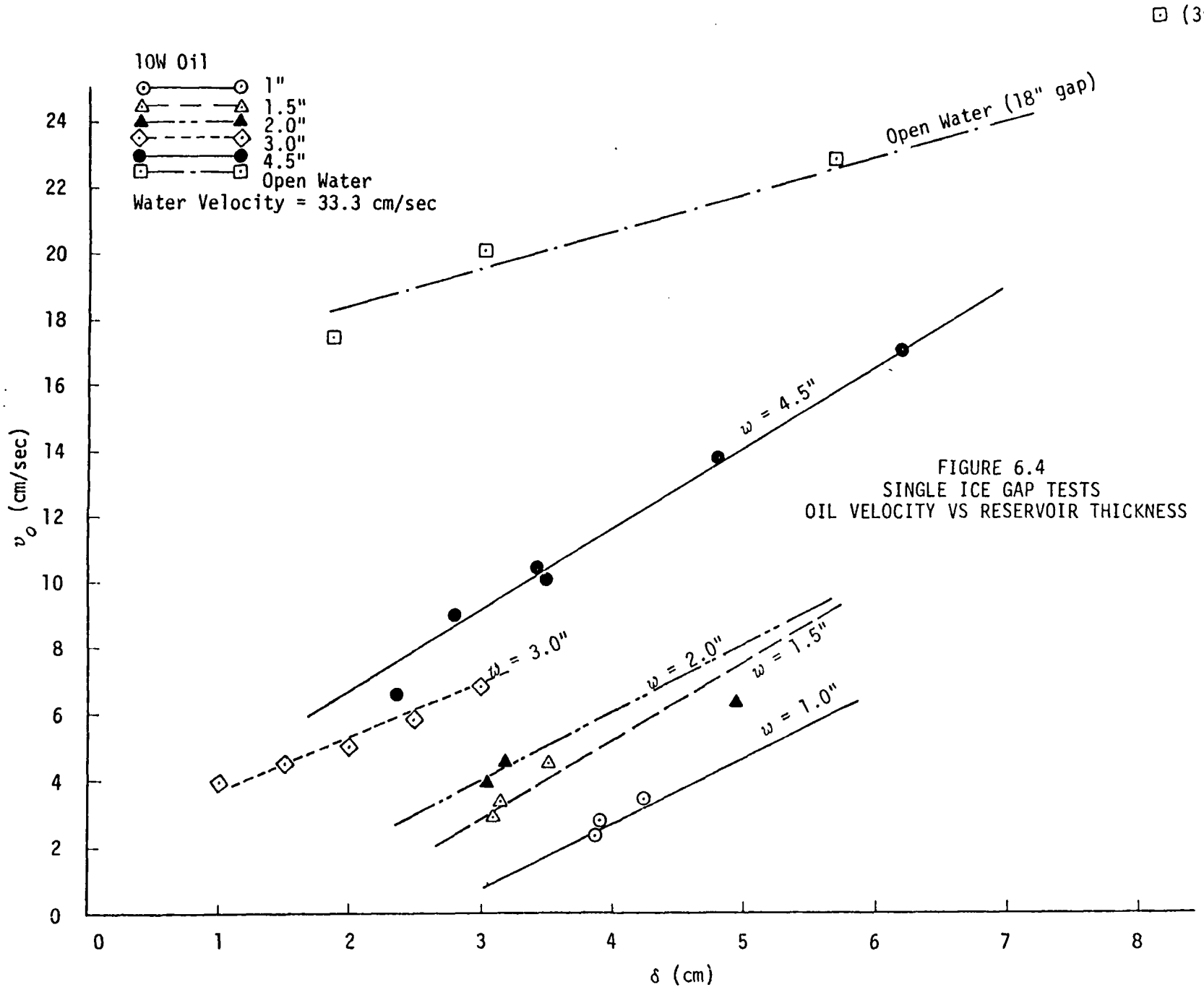

FIGURE 6.4
SINGLE ICE GAP TESTS
OIL VELOCITY VS RESERVOIR THICKNESS

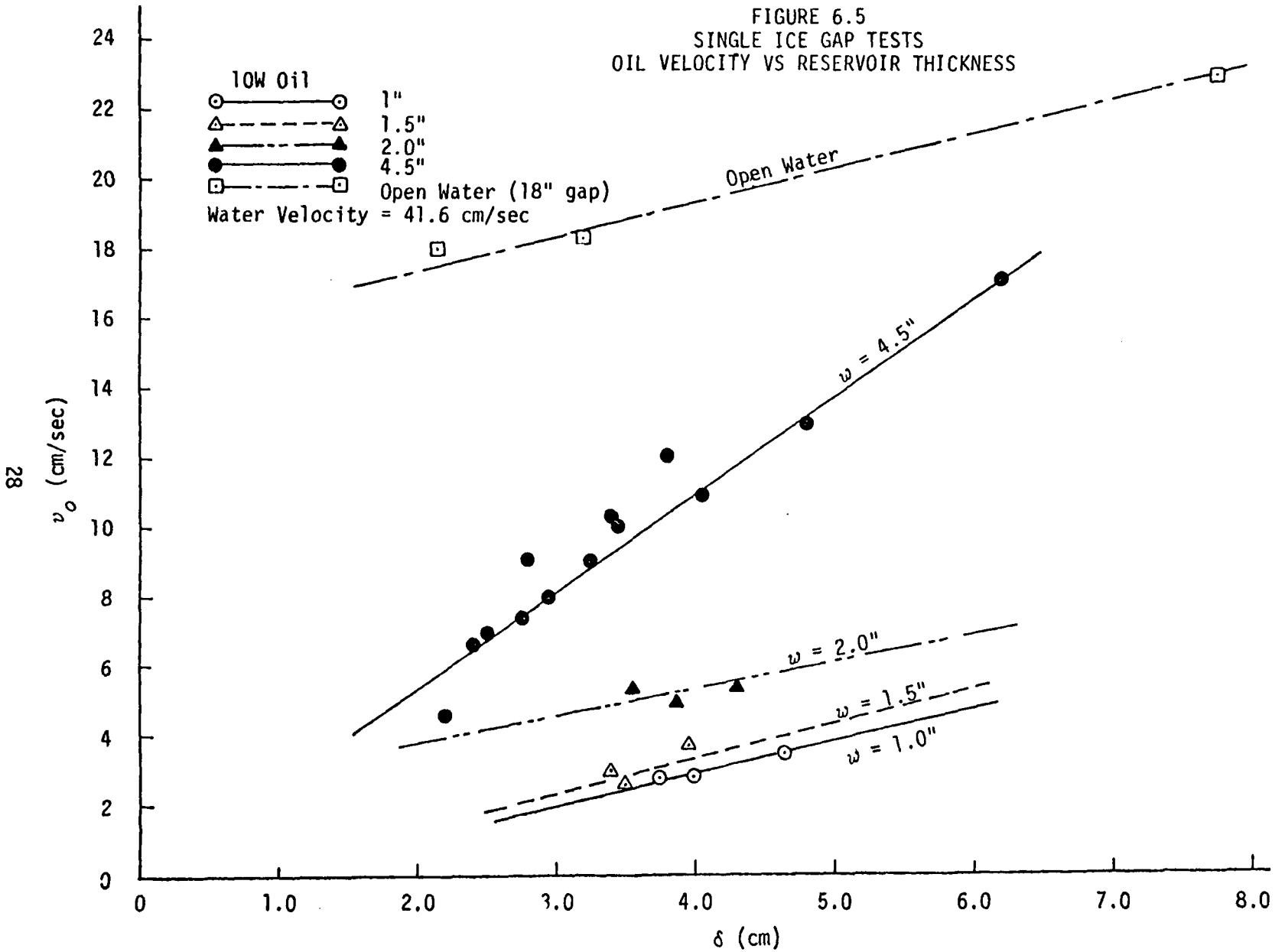

FIGURE 6.5
SINGLE ICE GAP TESTS
OIL VELOCITY VS RESERVOIR THICKNESS

The oil velocity data is plotted for a series of slick thickness to gap width ratios for SAE 10W oil in Figure 6.6. Figures 6.7 and 6.8 show the same information for the diesel fuel and the SAE 40W oil respectively.

From the data plots it appears that there is a linear relationship between the relative oil velocity and the representative terms for each of the forces acting on the oil as is portrayed by Equation (3.8). The curves for each slick thickness to gap width ratio for each oil type have approximately equal origin points and fan out with increasing slope for increasing slick thickness to gap width ratio. This indicates that a relationship exists between the slick thickness to gap width ratio and the slope of the curves. A single equation can be written to predict the oil velocity through a gap for each oil. The plots of equation slope versus thickness to gap width ratio are shown on Figure 6.9 for the SAE 10W oil, Figure 6.10 for the diesel fuel, and Figure 6.11 for the SAE 40W oil. The resulting equations for relative oil velocity through a gap for each oil tested are as follows:

$$\text{Diesel Oil: } \frac{v_o}{v_D} = 0.000034 \left(\frac{\delta}{\omega}\right)^{0.81} \left(\frac{Re}{Fr^2}\right)\left(\frac{\rho_o}{\rho_D}\right) + 0.015 \qquad (6.1)$$

$$\text{SAE 10W Oil: } \frac{v_o}{v_D} = 0.00089 \left(\frac{\delta}{\omega}\right)^{0.78} \left(\frac{Re}{Fr^2}\right)\left(\frac{\rho_o}{\rho_D}\right) + 0.00049 \qquad (6.2)$$

$$\text{SAE 40W Oil: } \frac{v_o}{v_D} = 0.0034 \left(\frac{\delta}{\omega}\right)^{0.45} \left(\frac{Re}{Fr^2}\right)\left(\frac{\rho_o}{\rho_D}\right) + 0.0028 \qquad (6.3)$$

By dimensionalizing these three equations, and substituting values for the oil properties and physical constants, equations which give the oil velocity through a gap as a function of the oil slick thickness, gap width and velocity of the driving fluid can be written as follows:

$$\text{Diesel Oil: } v_o = 0.41\ \delta^{0.81}\ w^{1.19} + 0.015\ v_D \qquad (6.4)$$

$$\text{SAE 10W Oil: } v_o = 0.22\ \delta^{0.78}\ w^{1.22} + 0.00049\ v_D \qquad (6.5)$$

$$\text{SAE 40W Oil: } v_o = 0.081\ \delta^{0.45}\ w^{1.55} + 0.0028\ v_D \qquad (6.6)$$

where v_o and v_D are measured in cm/s and δ and w are measured in centimeters.

6.3 Oil Seepage Through a Field of Broken Ice

When a thick pool of oil is released at the water surface, it quickly spreads over the water in a thin layer because of its unbalanced hydrostatic force. This spreading force will be exerted on any ice blocks encountered by the spreading oil. This force will tend to move the blocks in the direction of oil spread.

During the testing, oil was released from a thick reservoir into a random, unpacked, restrained ice field. The oil pushed the ice blocks forward

FIGURE 6.6
SINGLE ICE GAP TESTS
RELATIVE OIL VELOCITY VS DRIVING FORCE

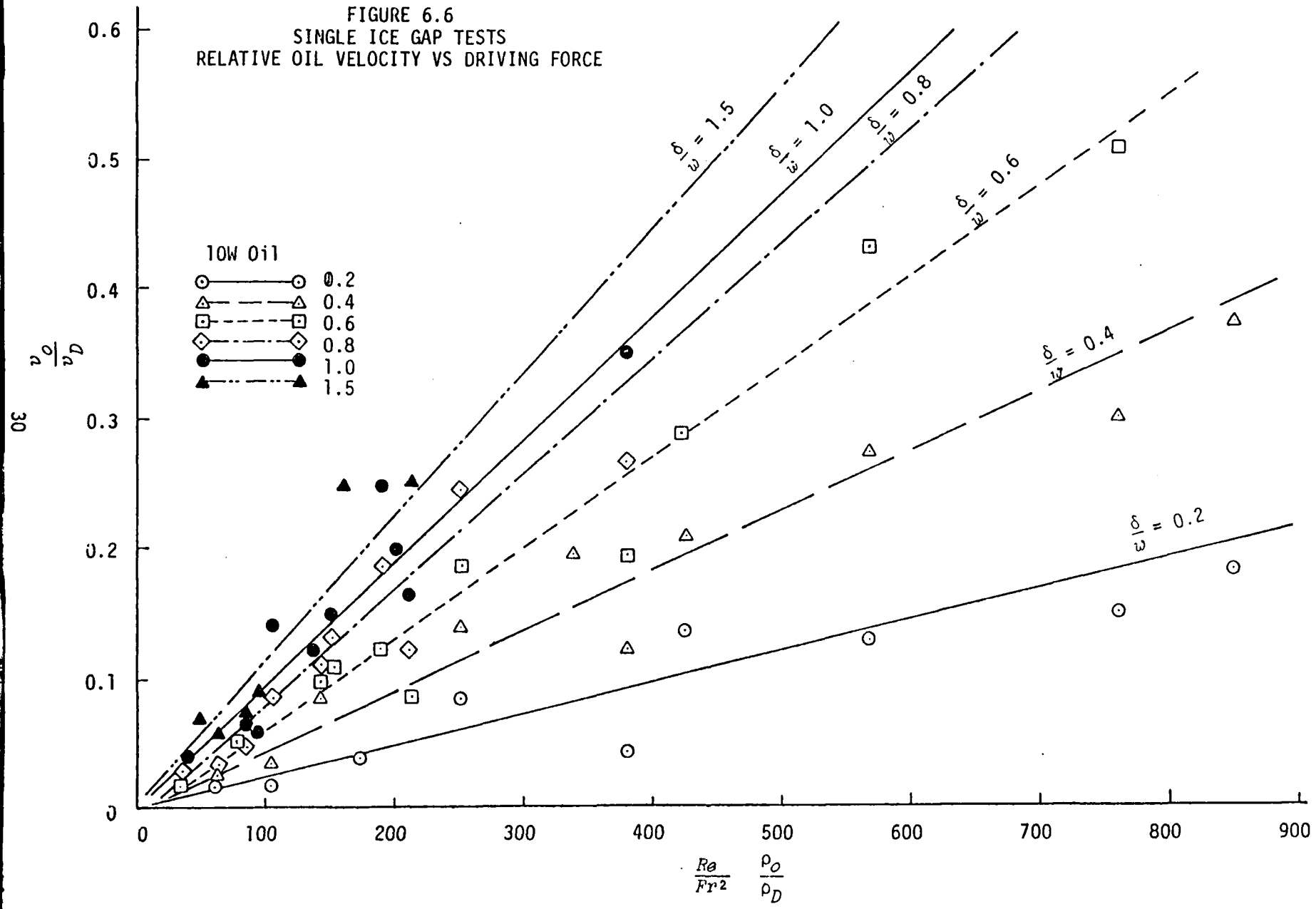

FIGURE 6.7
SINGLE ICE GAP TESTS
RELATIVE OIL VELOCITY VS DRIVING FORCE

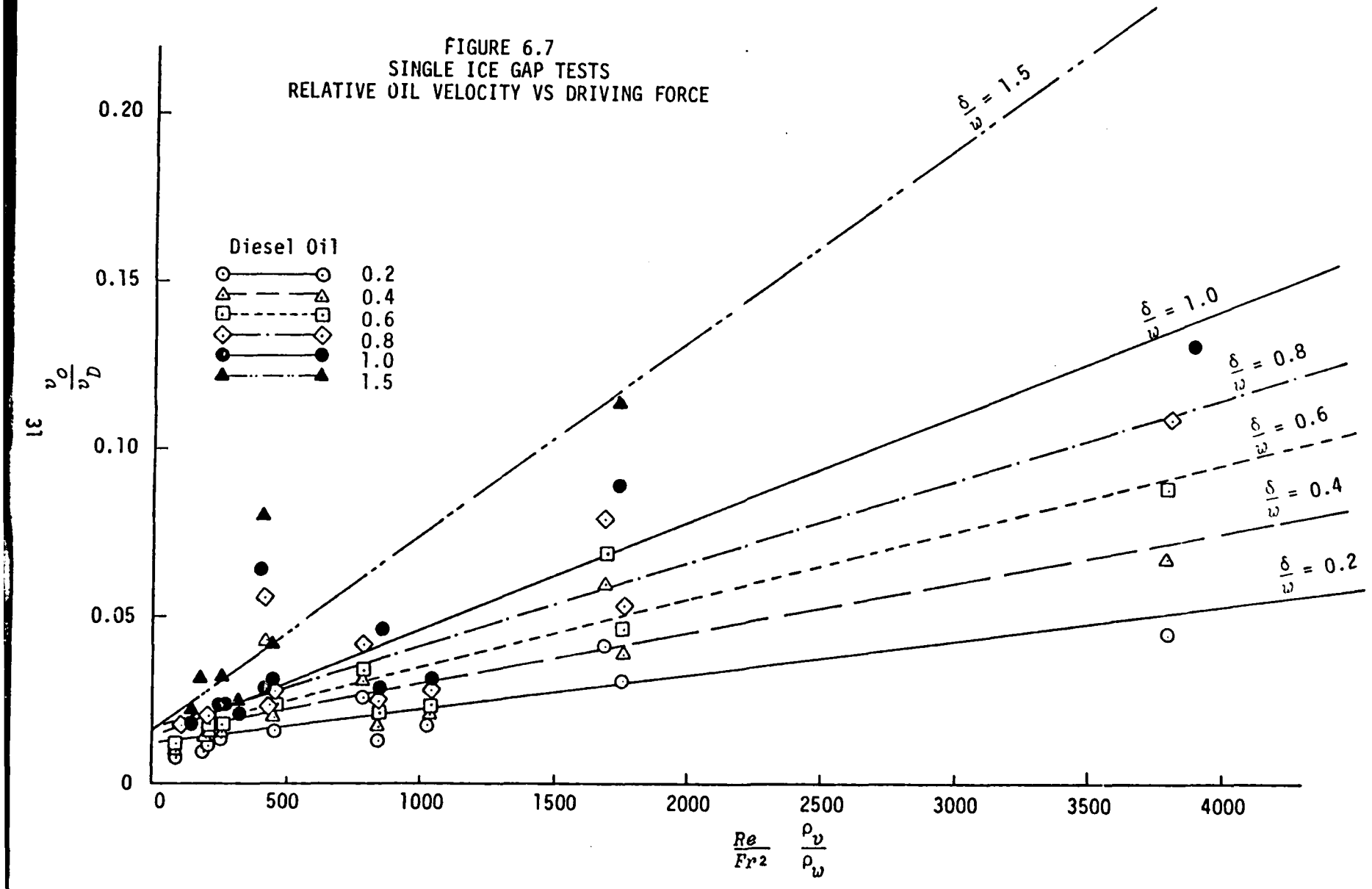

FIGURE 6.8
SINGLE ICE GAP TESTS
RELATIVE OIL VELOCITY VS DRIVING FORCE

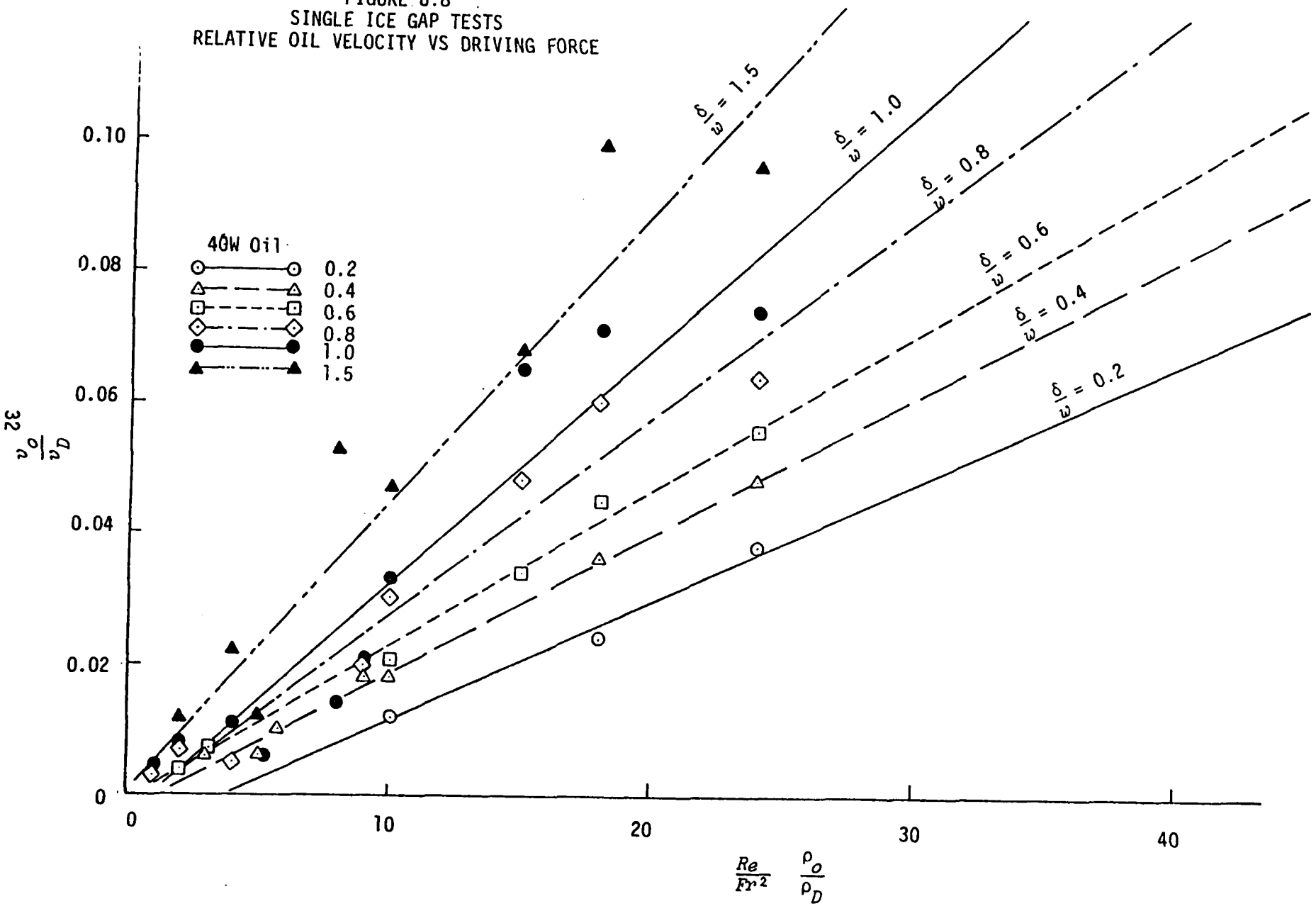

FIGURE 6.9
SLOPE OF RELATIVE OIL VELOCITY EQUATIONS VS
RELATIVE SLICK THICKNESS
10W OIL

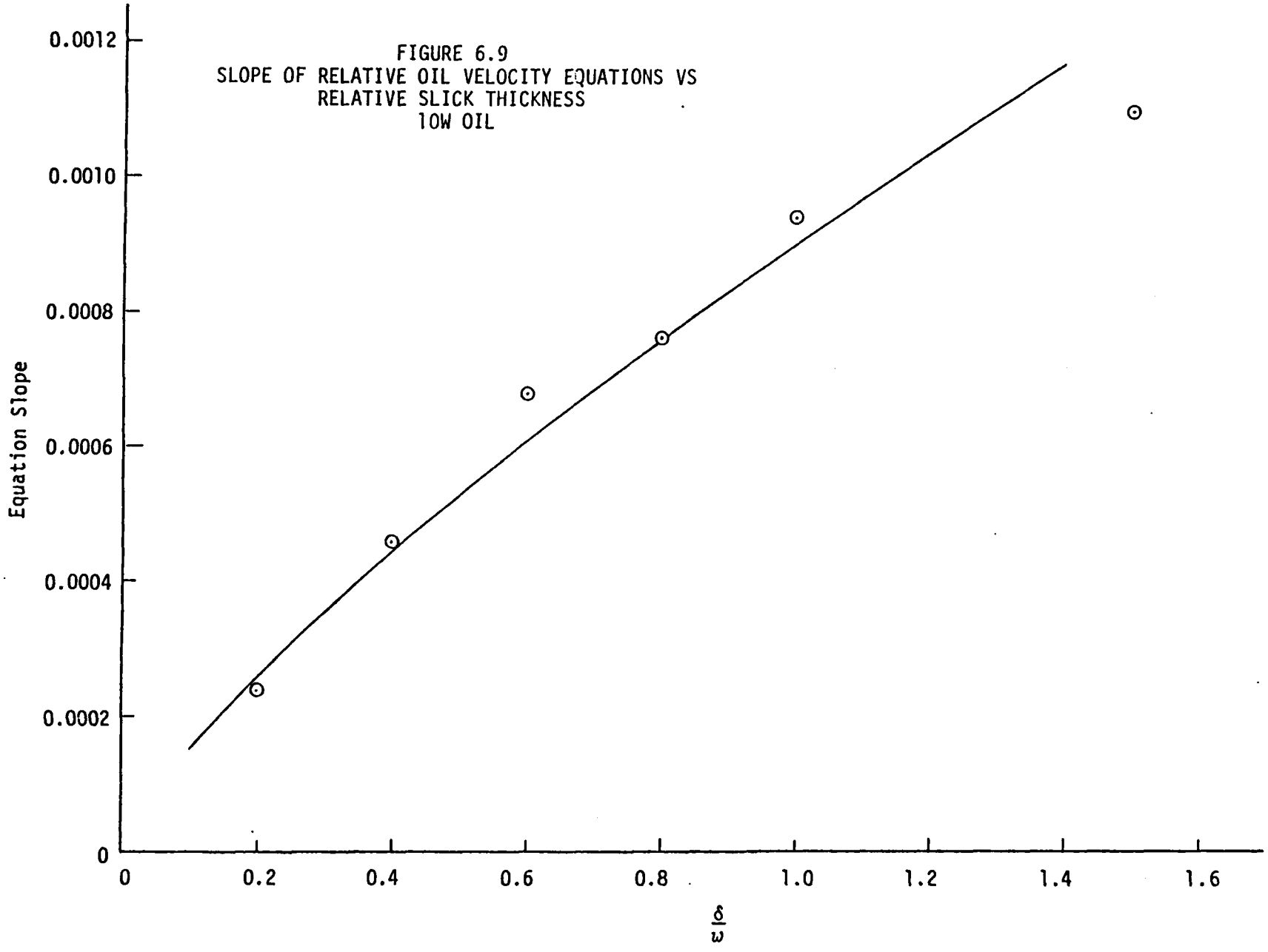

FIGURE 6.10
SLOPE OF RELATIVE OIL VELOCITY EQUATIONS VS
RELATIVE SLICK THICKNESS
DIESEL FUEL

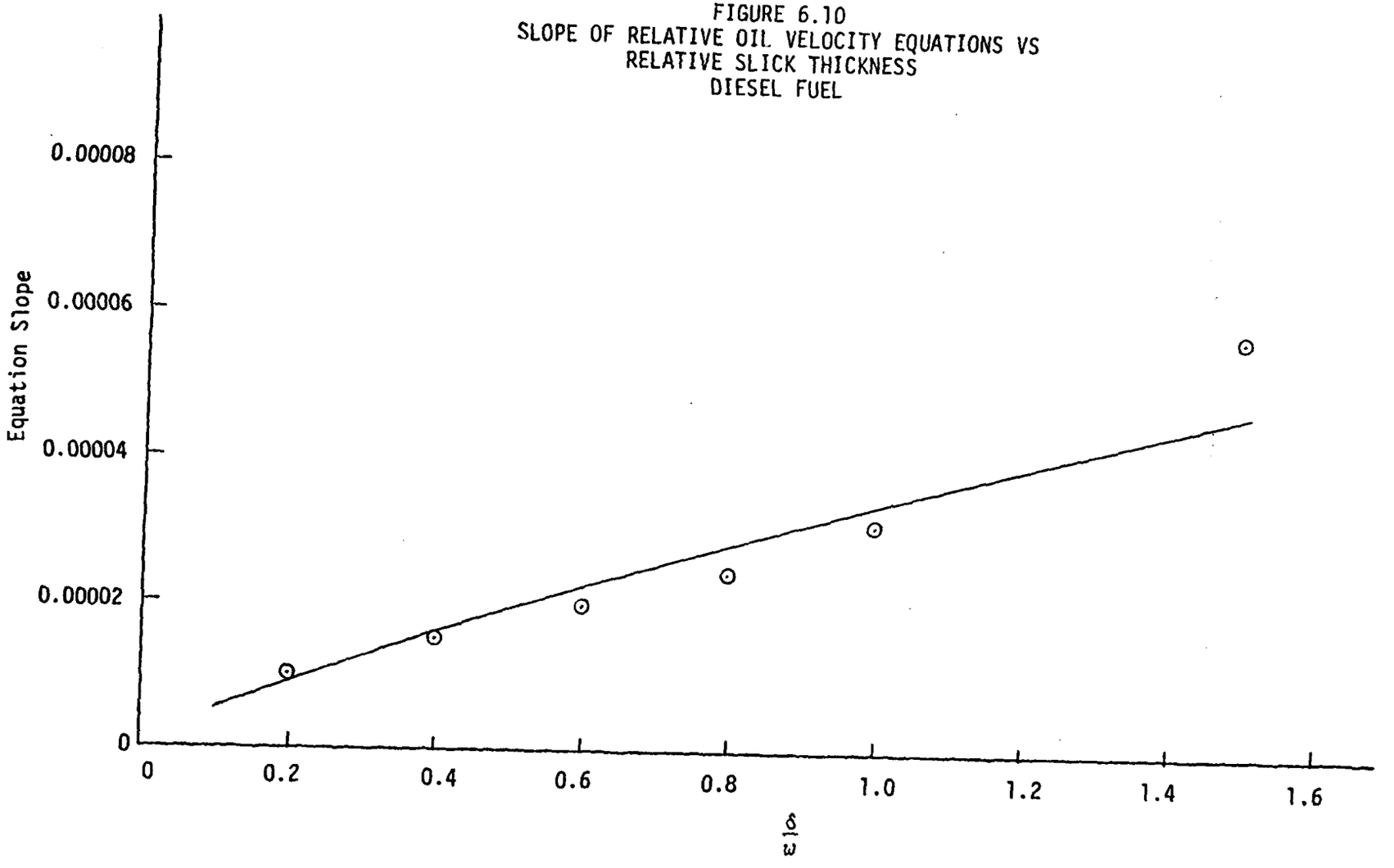

FIGURE 6.11
SLOPE OF RELATIVE OIL VELOCITY EQUATIONS VS
RELATIVE SLICK THICKNESS
40W OIL

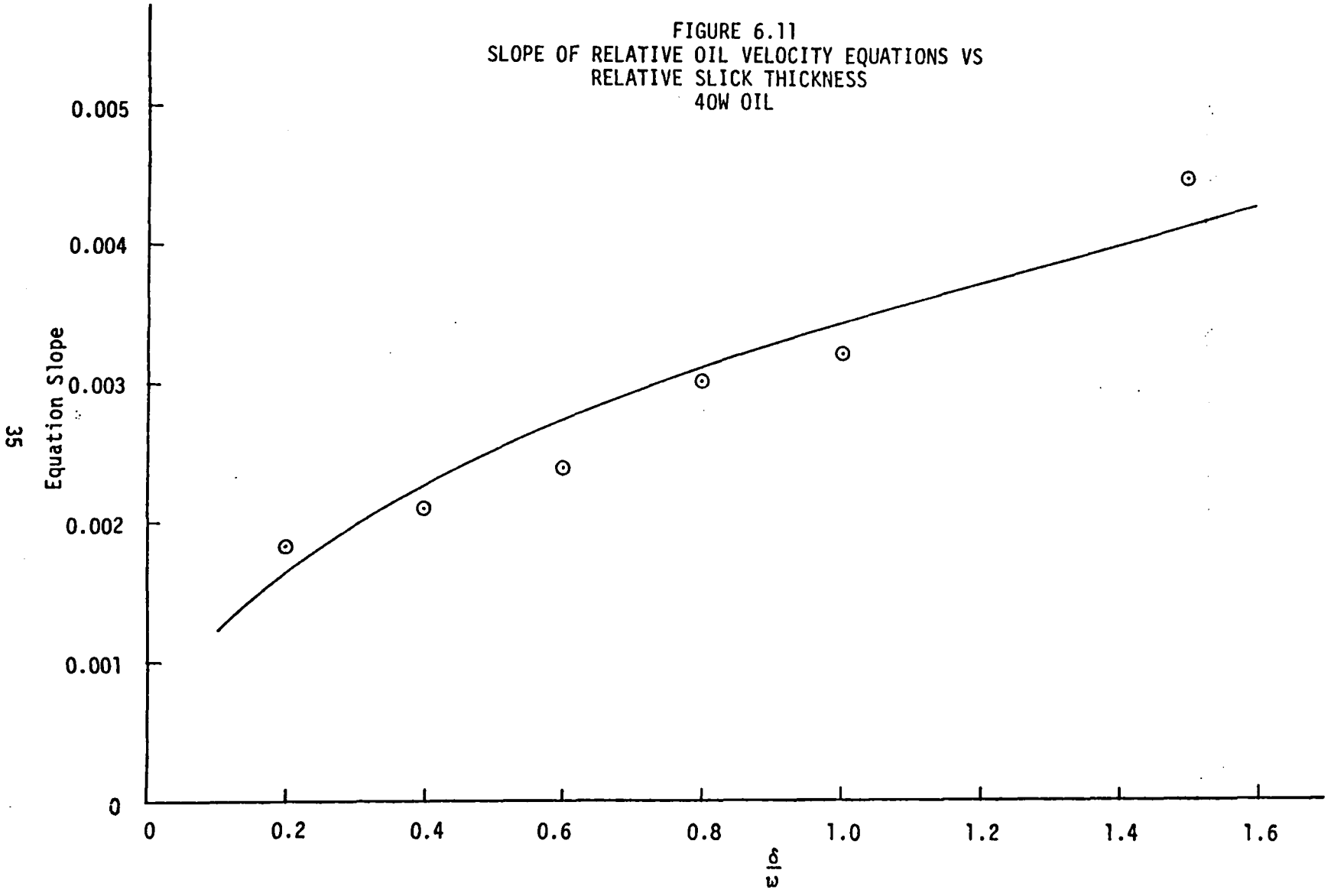

against the barrier to a compact high concentration ice field. At this high concentration, the gaps between the ice blocks were small. Whether or not an oil can seep through a packed field of broken ice at maximum concentration is determined by the thickness and viscosity of the oil. During the experimental program, only the diesel fuel was able to flow through the small gaps in the ice. The SAE 10W and SAE 40W oils were both too viscous to flow through the gaps, and were totally contained in the reservoir behind the ice.

The flow rate of the diesel fuel through the tightly packed ice field was determined by measuring the change in volume in the oil reservoir over time. The oil flowed through the ice pack in a very thin layer, meandering through the small gaps between the ice blocks. Equation (3.12), presented in Section 3.2.1, gives an expression for the seepage rate of oil through a broken ice pack as a function of the thickness of the oil in the reservoir and a characteristic dimension of the ice pack:

$$\frac{q^2}{g\, b^3} = K_3 \left(\frac{\delta}{b}\right)^{K_4} . \tag{3.12}$$

The values of the coefficients K_3 and K_4 are to be determined from the experimental data.

Equation (3.10), also presented in Section 3.2.1, is an expression for the ice pack characteristic dimension, b. This characteristic dimension is a function of the size of an individual ice block, d, and of the surface concentration of the ice field, c:

$$b = d \left(\frac{1}{\sqrt{c}} - 1\right) . \tag{3.10}$$

The ice concentration, c, is the ratio of the surface area of ice in the broken pack to the total surface area of the pack. During the laboratory testing the surface area of ice was determined by multiplying the area of an ice block by the known number of ice blocks in the pack. The overall dimensions of the ice pack were measured directly to give the total surface area. Typically, the 3.25 inch ice blocks had maximum observed concentrations in the range of 0.8 to 0.85, while the 6.5 inch size blocks had maximum observed concentrations of 0.85 to 0.90.

Because the ice block dimension dominates over the ice concentration in Equation (3.10), the large ice blocks typically had larger b values than the small ice blocks. However, since b is not a measure of the actual gaps that would exist in a randomly packed ice field, the oil flowrate through the ice pack did not necessarily vary directly with b, and large blocks did not necessarily allow higher oil seepage rates than small blocks.

Figure 6.12 is a plot of the oil seepage through broken ice data for the diesel fuel, non-dimensionalized to fit Equation (3.12). By means of a curve fitting technique, a best fit line has been drawn through the data. The equation for the line fitting this data is:

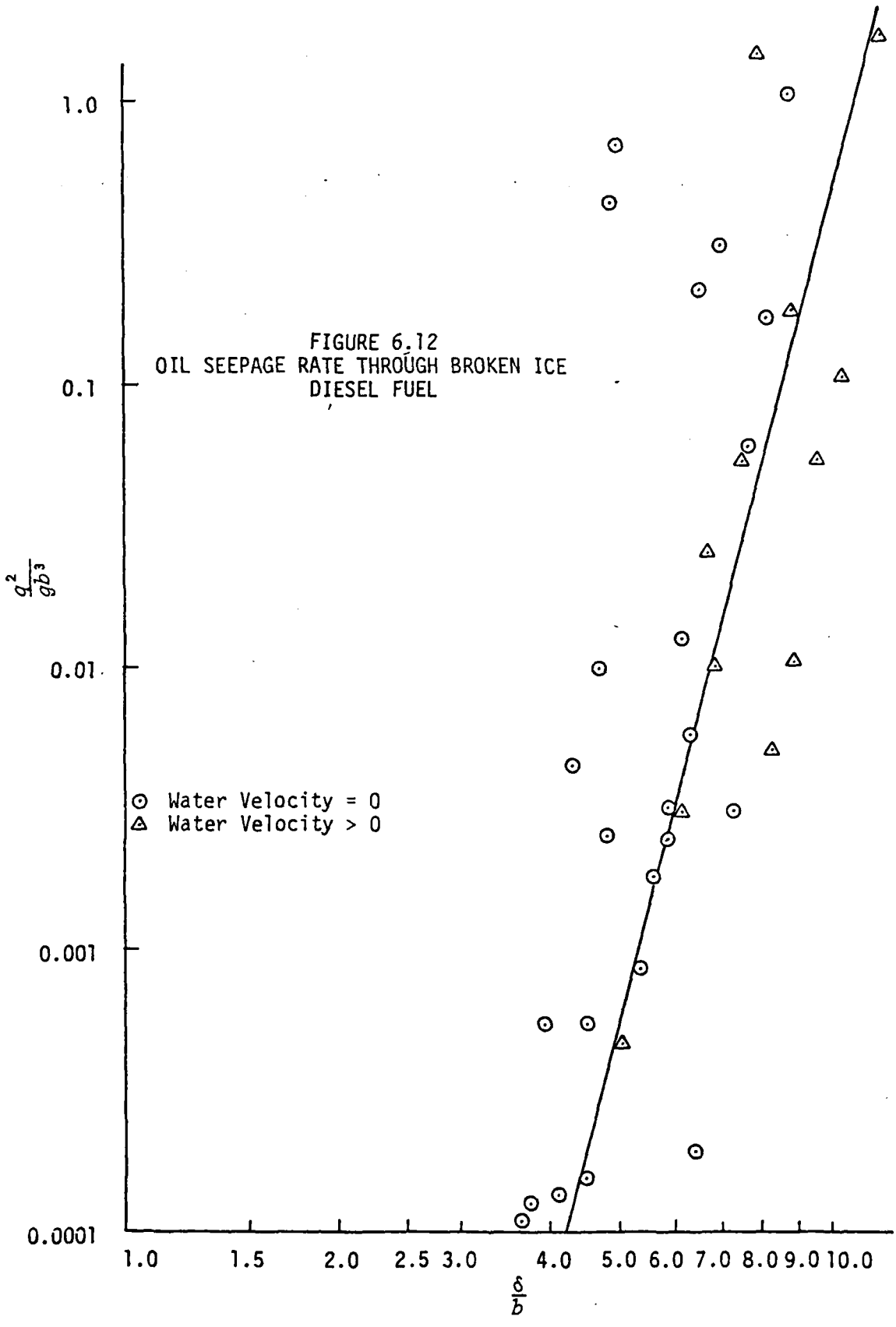

FIGURE 6.12
OIL SEEPAGE RATE THROUGH BROKEN ICE
DIESEL FUEL

$$\frac{q^2}{g\,b^3} = 6.92 \times 10^{-10} \left(\frac{\delta}{b}\right)^{8.73} \quad . \tag{6.7}$$

Note on Figure 6.12 that data from the static (no water velocity) and the current tests have been plotted together, and are both reasonably represented by Equation (6.7). This is proof of the previous discussion which stated that the seepage rate of oil through a restrained ice pack would be independent of the water current. The ice blocks are much thicker than the oil layer seeping through the field, therefore, the current is masked from the oil.

Although Equation (6.7) is useful from a non-dimensional point of view, an equation which directly gives the flowrate of oil per unit width through the broken ice would be more useful to on-site spill response personnel. The dimensional form of Equation (6.7), expressing the oil flowrate in gallons per minute per foot of width as a function of oil slick thickness in centimeters and the ice field characteristic dimension in inches, is:

$$q = 2.74 \times 10^{-5} \frac{\delta^{4.37}}{b^{2.87}} \quad . \tag{6.8}$$

Figure 6.13 shows Equation (6.8), where q is plotted against δ for a series of values for b.

6.4 Oil Interaction with a Moving Ice Field

When oil from a thick reservoir is released in a broken ice field that is free to move, the oil will exert a hydrostatic force on the ice pack and push it downstream. At the same time, small amounts of oil will seep into the broken ice field as was described in Section 6.3. The spread rate of the oil therefore is equal to the velocity of the ice field in front of the oil, plus the seepage rate of the oil through the ice field.

In Section 3.2.2 a relationship was developed for the velocity of the front of an ice field being pushed by a thick oil slick. The ice velocity was assumed to be directly proportional to the square of the oil thickness (driving force), and inversely proportional to the ice field thickness and length (resisting forces) as follows:

$$v_i = K_5 \left(\frac{\delta^2}{tl}\right) + K_6 \quad . \tag{3.11}$$

The constants K_5 and K_6 are assumed to be dependent upon the velocity of the water and the properties of the oil.

Tests of oil spilled in unrestrained ice fields were performed using several water velocities and two different oil types. The tests were performed using the small and large ice blocks both individually and combined. Figure 6.14 is a plot of the data obtained from the diesel fuel tests, and Figure 6.15 is a plot of the data from the SAE 10W oil tests. Equation (3.13) has been fit to the data for each oil and water velocity. The plot of these equations are shown on Figures 6.14 and 6.15. At small values of δ^2/tl (thin oil slicks)

FIGURE 6.13
FLOW RATE THROUGH BROKEN ICE VS OIL SLICK THICKNESS
DIESEL FUEL

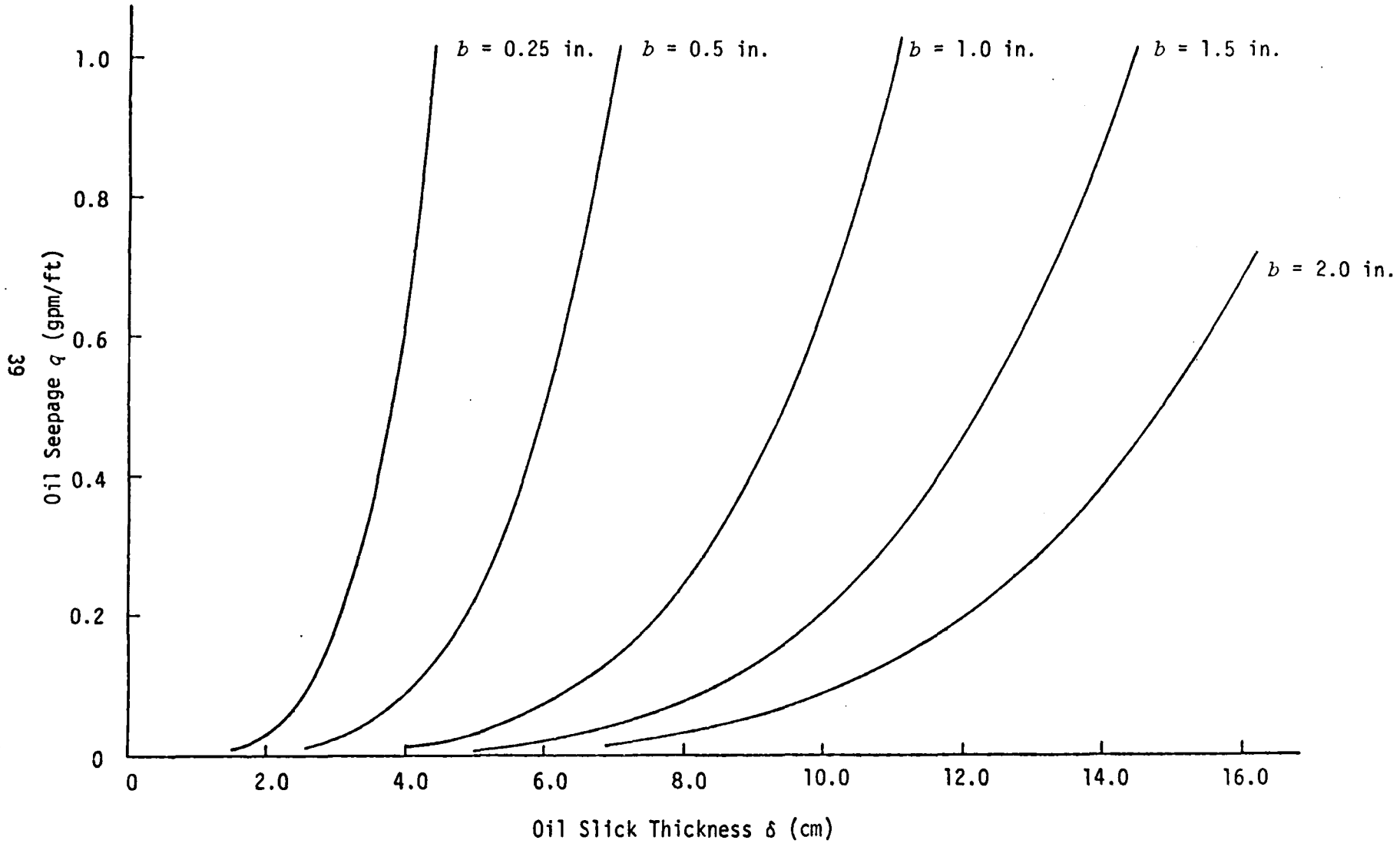

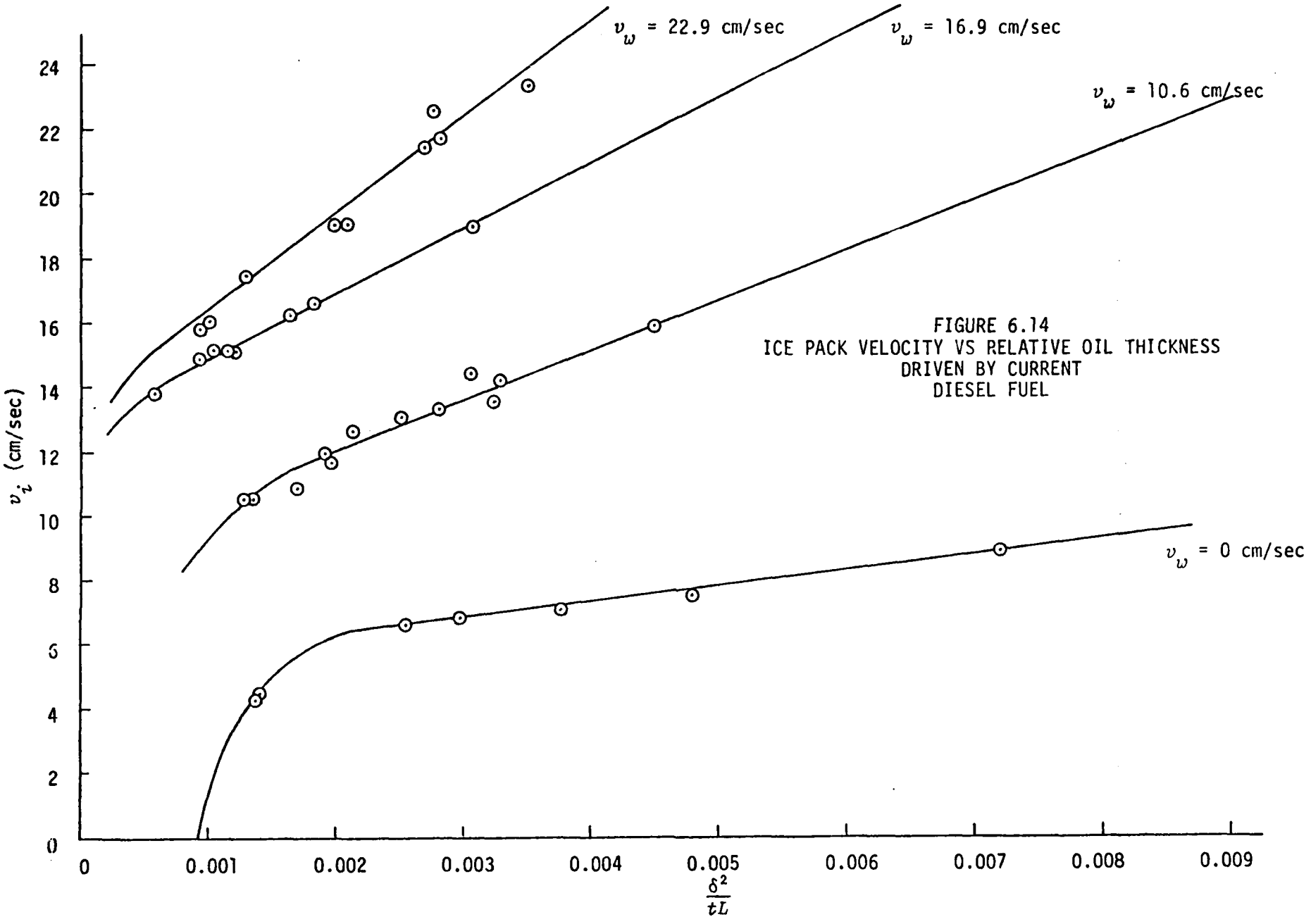

FIGURE 6.14
ICE PACK VELOCITY VS RELATIVE OIL THICKNESS
DRIVEN BY CURRENT
DIESEL FUEL

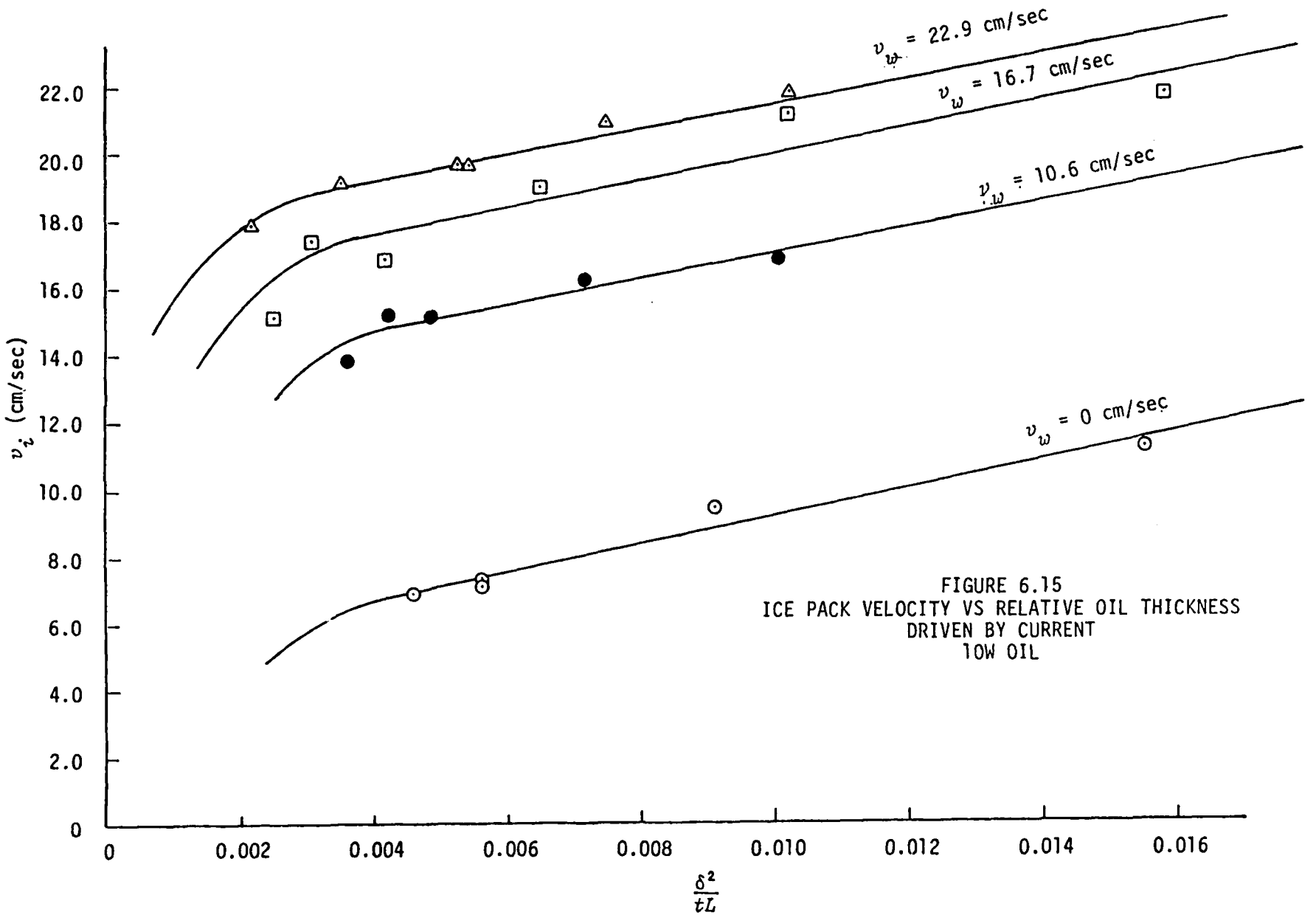

FIGURE 6.15
ICE PACK VELOCITY VS RELATIVE OIL THICKNESS
DRIVEN BY CURRENT
10W OIL

Equation (3.13) no longer applies because the driving force due to the oil becomes much less significant than the driving force due to the current. As this ratio decreases, the ice velocity decreases to the oil free ice velocity.

The relationships between the ice velocity and δ^2/tL which are plotted on Figure 6.14 for the diesel fuel are:

$$v_i = 489 \frac{\delta^2}{tL} + 5.35 \quad \text{for } v_w = 0 \tag{6.9a}$$

$$v_i = 1546 \frac{\delta^2}{tL} + 9.05 \quad \text{for } v_w = 10.6 \text{ cm/s} \tag{6.9b}$$

$$v_i = 2021 \frac{\delta^2}{tL} + 12.9 \quad \text{for } v_w = 16.7 \text{ cm/s} \tag{6.9c}$$

$$v_i = 3002 \frac{\delta^2}{tL} + 13.4 \quad \text{for } v_w = 22.9 \text{ cm/s} \tag{6.9d}$$

where v_i is in units of cm/s and δ, t, and L are in units of cm.

It appears from these equations that there is a relationship between the slopes of the equations and the velocity of the water, and a relationship between the intercepts of the equations and the velocity of the water. These relationships are plotted on Figure 6.16. The equations of these lines are:

$$\text{Equation Slope} = 106\ v_w + 433 \tag{6.10}$$

$$\text{Equation Intercept} = 0.376\ v_w + 5.44 \tag{6.11}$$

Combining Equations (6.10) and (6.11) with Equations (6.9a) through (6.9d) gives an expression for the velocity of a broken ice pack, behind which a quantity of diesel fuel has been spilled:

$$v_i = (106 \frac{\delta^2}{tL} + 0.376)\ v_w + 433 \frac{\delta^2}{tL} + 5.44 \tag{6.12}$$

where v_i is in units of cm/s and δ, t, and L are in units of cm.

This equation can be assumed to be applicable for values of δ^2/tL greater than or equal to 0.00175.

The relationships between ice velocity and δ^2/tL which are plotted on Figure 6.15 for the SAE 10W oil are:

$$v_i = 414 \frac{\delta^2}{tL} + 5.04 \quad \text{for } v_w = 0 \tag{6.13a}$$

$$v_i = 387 \frac{\delta^2}{tL} + 13.2 \quad \text{for } v_w = 10.6 \text{ cm/s} \tag{6.13b}$$

$$v_i = 401 \frac{\delta^2}{tL} + 16.0 \quad \text{for } v_w = 17.6 \text{ cm/s} \tag{6.13c}$$

$$v_i = 365 \frac{\delta^2}{tL} + 17.1 \quad \text{for } v_w = 22.9 \text{ cm/s} \tag{6.13d}$$

where v_i is in units of cm/s and δ, t, and L are in units of cm.

FIGURE 6.16
ICE PACK VELOCITY EQUATION SLOPE AND
INTERCEPT VS WATER VELOCITY
DIESEL FUEL

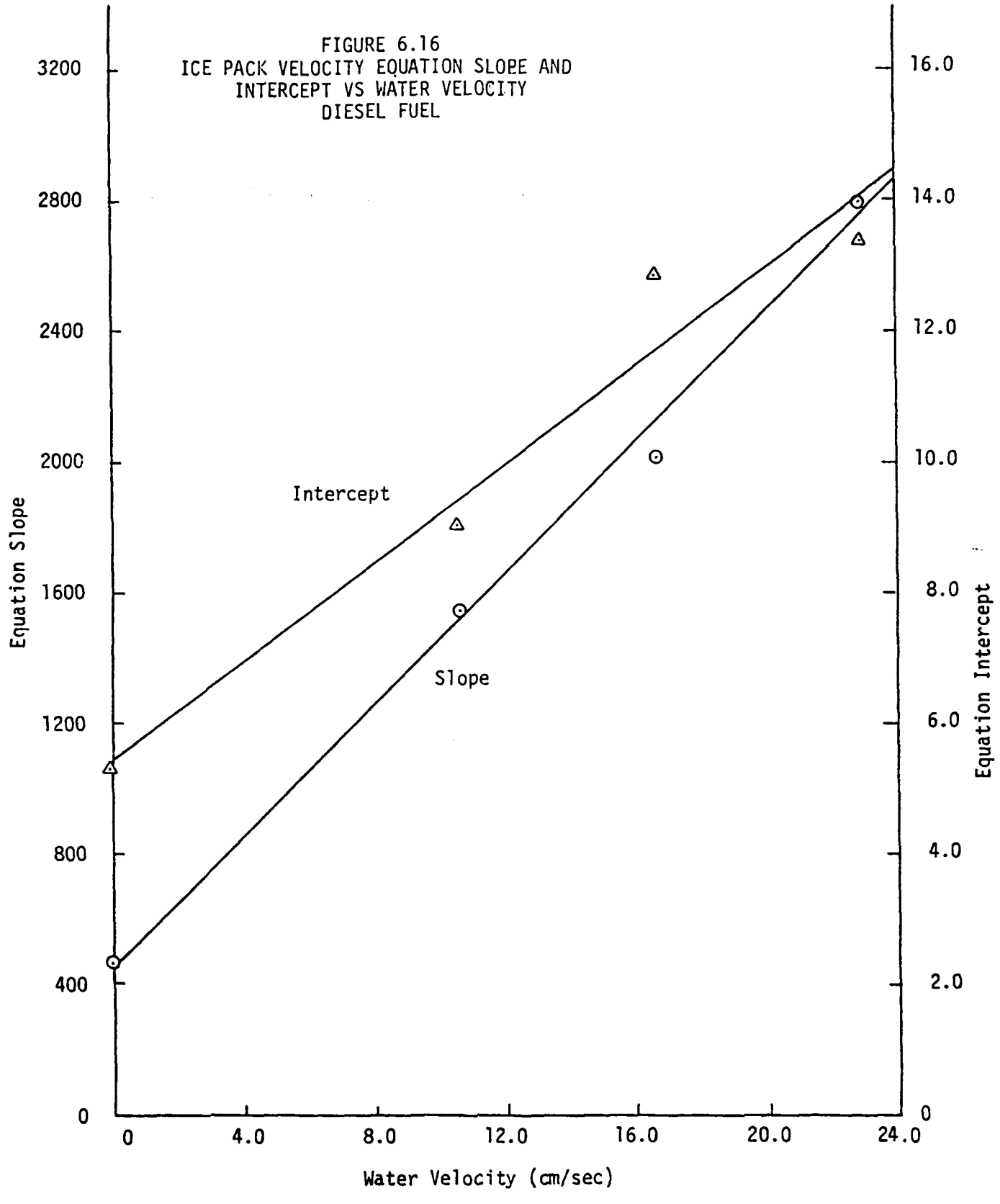

It appears from Equations (6.13a) through (6.13d) that there is a relationship between the intercepts of the equations and the water velocity. The slopes of the equations appear to be independent of the water velocity, and may best be represented by an average value. The relationship between the intercepts of Equations (6.13a) through (6.13d) and the water velocity is plotted on Figure 6.17. The equation for this relationship is:

$$\text{Equation Intercept} = 0.540\ v_w + 6.04\ . \qquad (6.14)$$

Combining Equations (6.13a) through (6.13d) with Equation (6.14) and using an average value for the equation slopes gives the following equation for the front velocity of a broken ice pack, behind which a quantity of SAE 10W oil has been spilled:

$$v_i = 0.504\ v_w + 392\ \frac{\delta^2}{tL} + 6.04\ . \qquad (6.15)$$

where v_i and v_w are in units of cm/s and δ, t, and L are in units of cm.

This equation can be assumed to apply for values of δ^2/tL greater than or equal to 0.004.

Tests of unrestrained ice fields interacting with diesel fuel were also run using the wind tunnel at several wind velocities. Figure 6.18 is a plot of the data that was obtained from these tests. A form of equation (3.13) has been fit to this data for each wind velocity and is plotted with the data on Figure 6.18.

From this test data, it can be seen that wind has much less influence on the movement of the ice and oil than the water current. It was not until the wind tunnel velocity approached 575 cm/s, corresponding to a 19 knot full-scale wind, that the results were significantly different from the zero wind velocity case. This implies that the roughness coefficient between the air and the ice is considerably less than that between the water and the ice.

The equations giving the relationship between ice velocity and δ^2/tL, which are shown on Figure 6.18 are:

$$v_i = 489\ \frac{\delta^2}{tL} + 5.35 \qquad \text{for } v_w = 0 \qquad (6.16a)$$

$$v_i = 586\ \frac{\delta^2}{tL} + 5.06 \qquad \text{for } v_w = 185 \text{ cm/s} \qquad (6.16b)$$

$$v_i = 464\ \frac{\delta^2}{tL} + 5.92 \qquad \text{for } v_w = 370 \text{ cm/s} \qquad (6.16c)$$

$$v_i = 368\ \frac{\delta^2}{tL} + 8.24 \qquad \text{for } v_w = 575 \text{ cm/s} \qquad (6.16d)$$

where v_i is in units of cm/s and δ, t, and L are in units of cm.

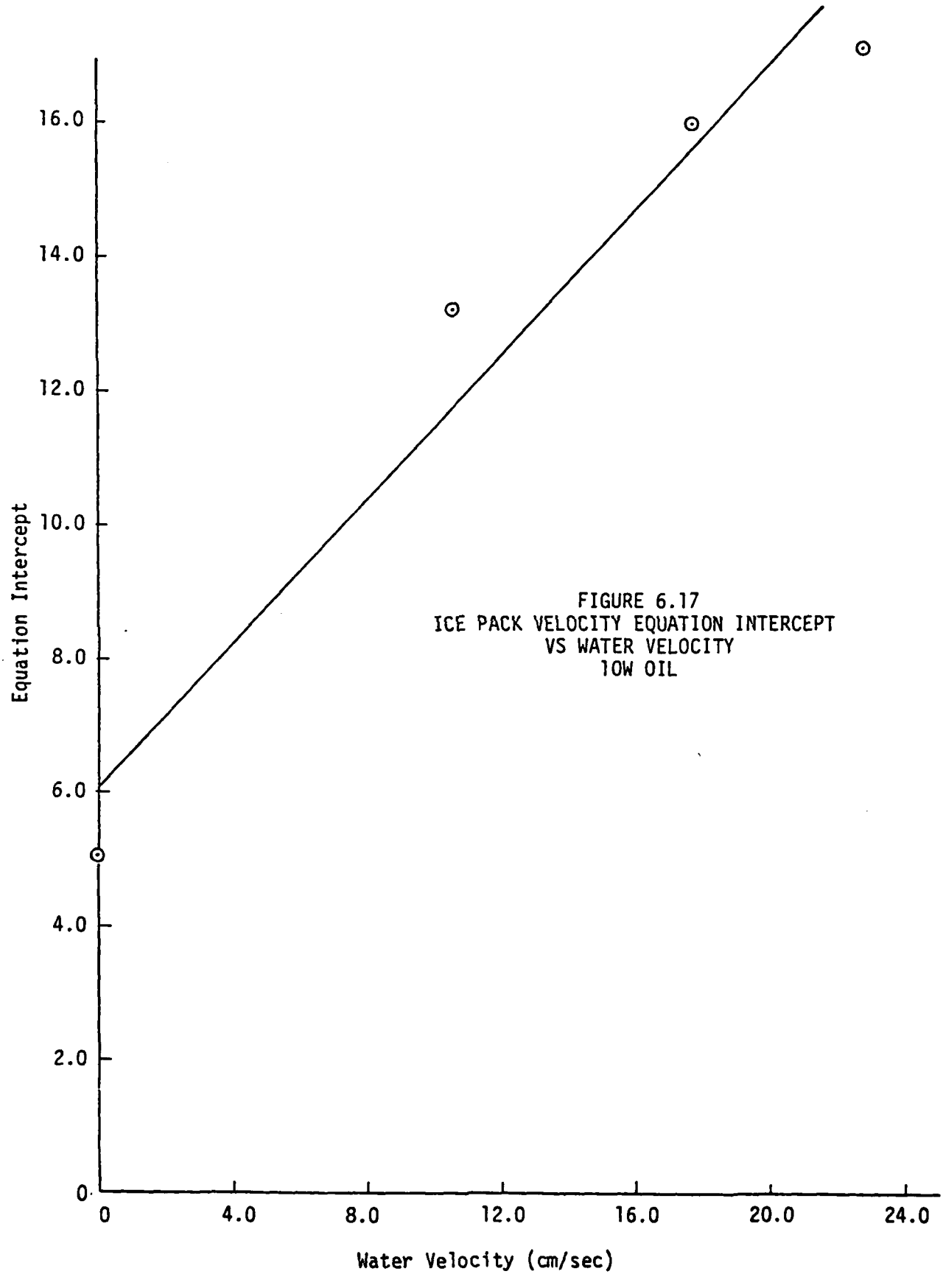

FIGURE 6.17
ICE PACK VELOCITY EQUATION INTERCEPT
VS WATER VELOCITY
10W OIL

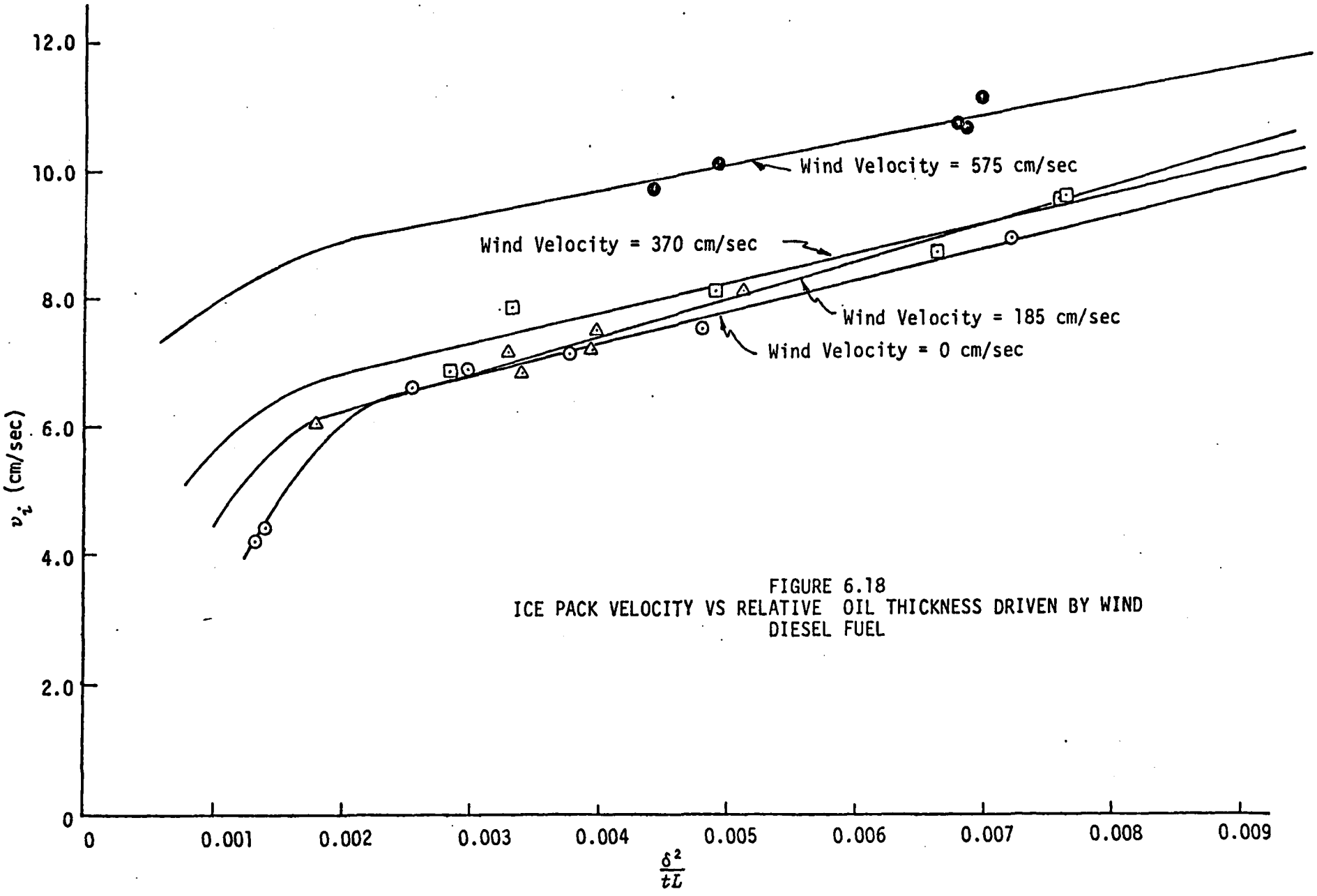

FIGURE 6.18
ICE PACK VELOCITY VS RELATIVE OIL THICKNESS DRIVEN BY WIND
DIESEL FUEL

From Equations (6.16a) through (6.16d) and from Figure 6.18, there does not appear to be any correlation between the wind velocity and the slopes or intercepts of the equations. The wind does not exert a significant driving force on the oil or the ice until its velocity is greater than approximately 500 cm/s. For velocities slightly below 500 cm/s the wind will only play a significant role when δ^2/tL decreases below 0.004. A single expression may be written to determine the ice velocity, independent of wind velocity for wind velocities less than 500 cm/s, corresponding to 16.4 knots full-scale:

$$v_i = 533 \frac{\delta^2}{tL} + 5.32 \quad , \tag{6.17}$$

where v_i is in units of cm/s and δ, t, and L are in units of cm. This equation corresponds to Equation (6.12) for the case where $v_w = 0$ with the exception that the linear regression analysis results in somewhat different coefficients.

It appears that a relationship similar to Equation (6.12) may be written to relate ice velocity to wind velocities greater than 500 cm/s, however, the wind tunnel built for this project was not designed to produce velocities in excess of 625 cm/s. Therefore, no data at higher speeds could be obtained.

7. APPLICATION OF RESULTS

As was stated in the introduction to this report, one of the major purposes of this study is to provide insight into how an oil slick spilled in an area of broken ice will act in the short-term. Such knowledge will allow on-scene spill response personnel to assess an oil spill in broken ice, and to choose the optimal containment and cleanup alternatives. This study has identified the underlying physics of oil movement and has evaluated the empirical constants from data obtained in small scale laboratory studies. Acknowledging a need for additional testing on a larger scale to determine the possible effects of scale or size, the following is a recommended step-by-step approach for predicting the spreading of an oil spill through broken ice, based upon a current best estimate of the oil flow phenomena. It is emphasized that the governing relationships will likely change as additional data is collected and further insight into the governing physical phenomena is obtained, however, taking the approach that it is desirable to develop a current best estimate on the basis of the current state of knowledge, the following procedure is recommended.

1. Determine the properties of the spilled oil (approximate density and viscosity if not known), and the size and thickness of the oil slick. The spread rate of the spilled oil is primarily a function of the oil properties and the slick thickness. The oil density and thickness dictate the hydrostatic force which is the driving force behind the spreading of the oil. The viscosity of the oil is the controlling factor in determining oil seepage through the gaps between the ice blocks. In general, the smaller the density and viscosity of the oil and the greater the oil slick thickness, the greater the spread rate of the spilled oil.

2. Determine the size and concentration of the broken ice field, the approximate dimensions of the broken ice pieces, and whether the ice field is restrained or free to move. The seepage rate through the ice field will depend upon the size of the ice pieces and the ice concentration. These two parameters are used to determine the ice pack characteristic dimension given by Equation (3.8). The oil seepage rate through broken ice varies inversely with this dimension. A restrained ice field will provide more oil containment than an ice field which is free to move. Oil spreads through a restrained ice field by seeping through the gaps between the ice pieces. Oil spreads through an unrestrained ice field by seeping through the gaps, as with the restrained ice field, but it also spreads behind the unrestrained field as the ice is pushed downstream by the hydrostatic force of the oil. If the ice field is restrained, only the light, low viscosity oils will seep through the ice field. Equation (6.8) and Figure 6.13 give the spread rate of diesel fuel through a restrained field of broken ice.

3. Determine the velocity of the underside currents or of the wind. If the broken ice field is restrained, the ice will mask the oil from the wind or current, and there will be no effect on the spreading of the oil. If the ice field is free to move, both the oil and the underside current will push the ice pack, and the oil will spread behind the ice field. The spread velocity of the oil will be equal to the ice pack velocity plus the seepage velocity of the oil. The ice pack velocity can be determined from Equation (6.12) for diesel fuel, or from Equation (6.15) for SAE 10W oil. High winds, approximately greater than 20 knots, will also effect the ice pack velocity and oil spread rate. Lesser winds have little effect on the oil spread velocity. Figure 6.18 can be used to determine the ice pack velocity and, therefore, the oil spread rate of diesel oil under wind conditions.

8. RECOMMENDATIONS

The results of this study provide considerable insight into the behavior of oil spilled in a broken ice field. The equations developed as part of this study match the data that was obtained in the ice flume tests and useful empirical relationships were obtained, with the intent that they could be used in modeling short term spill behavior and in providing guidance to spill response personnel in the field. There are, however, limitations to the results of this study. It is recommended therefore that the following work be considered to further refine and expand the results of this study.

1. Because the tests were performed in the relatively narrow Ice Flume, the results of this study are one-dimensional. While many spill situations will be one-dimensional, such as in leads or ship channels, there are also important situations, such as during breakup, where an oil spill in a field of broken ice will be two-dimensional,with the oil spreading in all directions from the location of the spill. It is recommended that additional testing be performed in ARCTEC's 100 x 12 foot Ice Basin where two dimensional oil spreading phenomena may be studied. Since it was determined that wind is much less significant than current in influencing oil spill spreading, it is recommended that two-dimensional wind tests be foregone in favor of more extensive current testing.

2. The mathematical expressions presented in this report are empirical and have not been generalized to the extent that they may be used in all situations. An effort should be made to refine these expressions by including additional terms, in order that they may be made more general in accurately predicting oil spill behavior in broken ice fields. This effort will require the conduct of additional tests in ARCTEC's Ice Flume covering an expanded array of system parameters.

3. The behavior of oil spilled in broken ice fields appears to be a phenomena which will yield itself well to mathematical modeling. A fairly complete model which would use the results of this study and the recommended additional studies could be developed at a reasonable cost. The mathematical model could then be used to develop realistic oil spill scenarios, and could additionally be used for training personnel in oil spill response procedures. The output of the model would include threshold of motion plots similar to those shown in Figure 6.1, seepage curves to allow cleanup personnel to determine the oil flow rate where oil seepage will occur, and a series of curves specifying the oil velocity as a function of the ice pack parameters and the wind and water velocities.

4. The empirical constants derived in this report could be subject to scale effects and one dimensionality effects. Experimental data based on controlled field experiments performed under actual arctic conditions would be most valuable in addressing concerns associated with scale effects. Such controlled field experiments are strongly recommended.

9. REFERENCES

1. Arya, S., "Air Friction and Form Drag on Arctic Sea Ice," AIDJEX Bulletin No. 19, March 1979.

2. Cox, J. C., L. A. Schultz, R. P. Johnson, and R. A. Shelsby, "The Transport and Behavior of Oil Spilled In and Under Sea Ice," ARCTEC, Inc. Report 460C, September 1980.

3. Hoult, D. P., In Oil on the Sea, ed. D. P. Hoult, pp. 65-80, 1969.

4. Hoult, D. P., "Oil Spreading on the Sea," Annual Review of Fluid Mechanics, 1972.

5. Schultz, L. A., "Tests of Oil Recovery Devices in Broken Ice Fields," United States Coast Guard Report CG-D-55-76, January 1976,

6. Sowers, G. B. and G. F. Sowers, Introductory Soil Mechanics and Foundations, Third Edition, MacMillan and Co., New York, 1970.

7. Uzuner, M. S., F. B. Weiskopf, J. C. Cox, L. A. Schultz, "Transport of Oil Under Smooth Ice Cover," United States Environmental Protection Agency, EPA-600/3-79-041, April 1979.

APPENDIX A

TEST EQUIPMENT

A.1 ARCTEC, Incorporated's Ice Flume

The experiments performed for this study were conducted in ARCTEC's insulated glass-walled Ice Flume. A sketch of the flume is presented as Figure A.1. The test section of the flume is 13.7 m long, 0.94 m wide, and 0.61 m deep. The flume is located in ARCTEC's insulated low temperature ice laboratory. The discharge capacity of the flume is approximately 140 liters per second at a water depth of 40 cm. This is achieved with a 25 cm axial flow pump, powered by a 10 horsepower variable speed motor. The discharge is measured by an annubar flow sensor connected in parallel with two eagle eye flow meters which measure the flow rate directly in gallons per minute. The maximum operating water depth of the flume is 46 cm, leaving approximately 15 cm of freeboard.

A.2 Wind Tunnel

To conduct the experiments examining wind effects on oil/broken ice interaction, a wind tunnel was built over ARCTEC's Ice Flume. The wind tunnel consisted of a series of 0.15 m high by 0.94 m wide by 1.52 m long interlocking sections which fit inside the rails of the flume. The sections were constructed of plywood, with the exception of one section which was made of clear plexiglass for observation and photography purposes. The wind tunnel was powered by a 15 inch blower with a 0.75 hp variable speed motor, fitted with a variable belt drive system. Wind speeds up to 550 cm/s were achievable through the tunnel with a water depth of 46 cm. Wind speed was measured by means of an anemometer.

A.3 Viscometer

A Brookfield Model LVT Synchrolectric Viscometer was used to measure apparent viscosity. The viscometer operates by rotating a cylinder or disk in the fluid and measuring the torque necessary to overcome the viscous resistance to movement. This is accomplished by driving the immersed element, which is called a spindle, through a beryllium copper spring. The degree to which the spring is wound, which is indicated by the position of a pointer on the viscometer dial, is proportional to the viscosity of the fluid for any given speed of rotation and spindle. For a material of given viscosity, the drag will be greater as the spindle size or the rotational speed increases. The minimum viscosity ranges are measured by using the largest spindle at the highest speed, and the maximum viscosity ranges are measured using the smallest spindle at the slowest speed. The viscosity measurement procedures used are in accordance with ASTM specification D 2983-72.

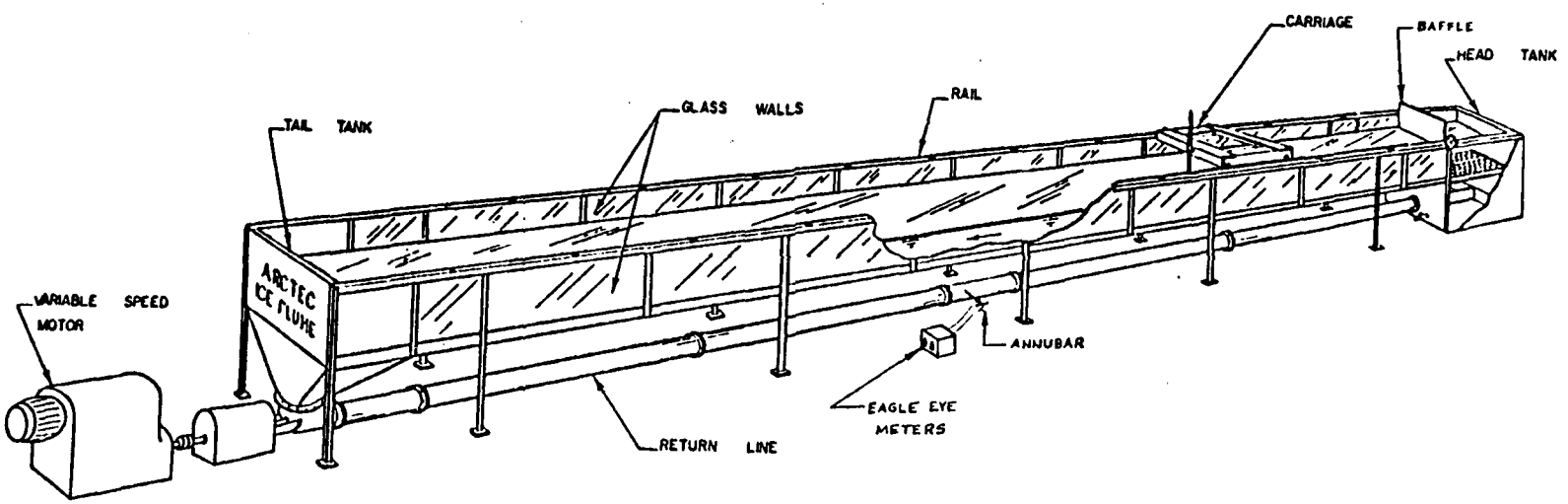

FIGURE A.1 INSULATED GLASS-WALLED ICE FLUME

A.4 Flow Measuring Devices

The annubar flow sensor is an annular averaging velocity head sensor specifically designed for the measurement of flow through a pipe. It measures differential pressure which is proportional to the square of the fluid velocity, and causes little permanent pressure loss. The annubar sensor is accurate to 1.0% of the actual velocity value, and is repeatable to 0.1% of this actual value.

The annubar may be installed in any plane of the pipe, whether vertical, horizontal, 45° or any angle in between. Consideration must be given, however, to the type of fluid which must be measured and the secondary instrumentation. For a liquid flowing through a horizontal pipe, such as is the case with ARCTEC's Ice Flume, it is best to install the annubar in the bottom or side of the pipe so that the instrument connections are below the pipe centerline. This ensures that the instrument lines are full of liquid and not air.

To complete the water flow sensing device, the annubar is connected in parallel with two eagle eye flow meters. These precalibrated meters are accurate and are repeatable to 1.5% of full-scale. Model 6000B has a scale of 0 to 1200 gpm, read in 20 gpm increments, and Model 6004B has a scale of 0 to 4000 gpm, read in 50 gpm increments. The meters are mounted below the annubar instrument lines as prescribed to ensure that no air is introduced into the meters.

Wind velocity is measured by means of a rotating anemometer. The anemometer is installed in the last wind tunnel section and is suspended so that it is in the approximate center of the air stream. The anemometer measures rotational displacement, which when measured for a given period of time, may be converted directly to wind speed.

A.5 Flume Work Carriage

The work carriage, shown on Figure A.2, served a dual purpose during the test program. A Milliken camera was mounted on the carriage to obtain overhead movies of the advancing oil and ice. The carriage was also used to measure the velocity of the ice field or oil slick. A pointer bar was attached to the work carriage for this purpose. By keeping the pointer bar aligned with the leading edge of the ice field or the oil slick, the position could be followed. Velocities could then be determined by means of a DC tach generator which was fastened to the wheel assembly of the carriage. The shaft of the tach generator was installed in contact with the carriage wheel and rotated as the carriage wheel turned, thus producing a signal which was proportional to velocity. This signal was read by a light pen oscillograph recorder.

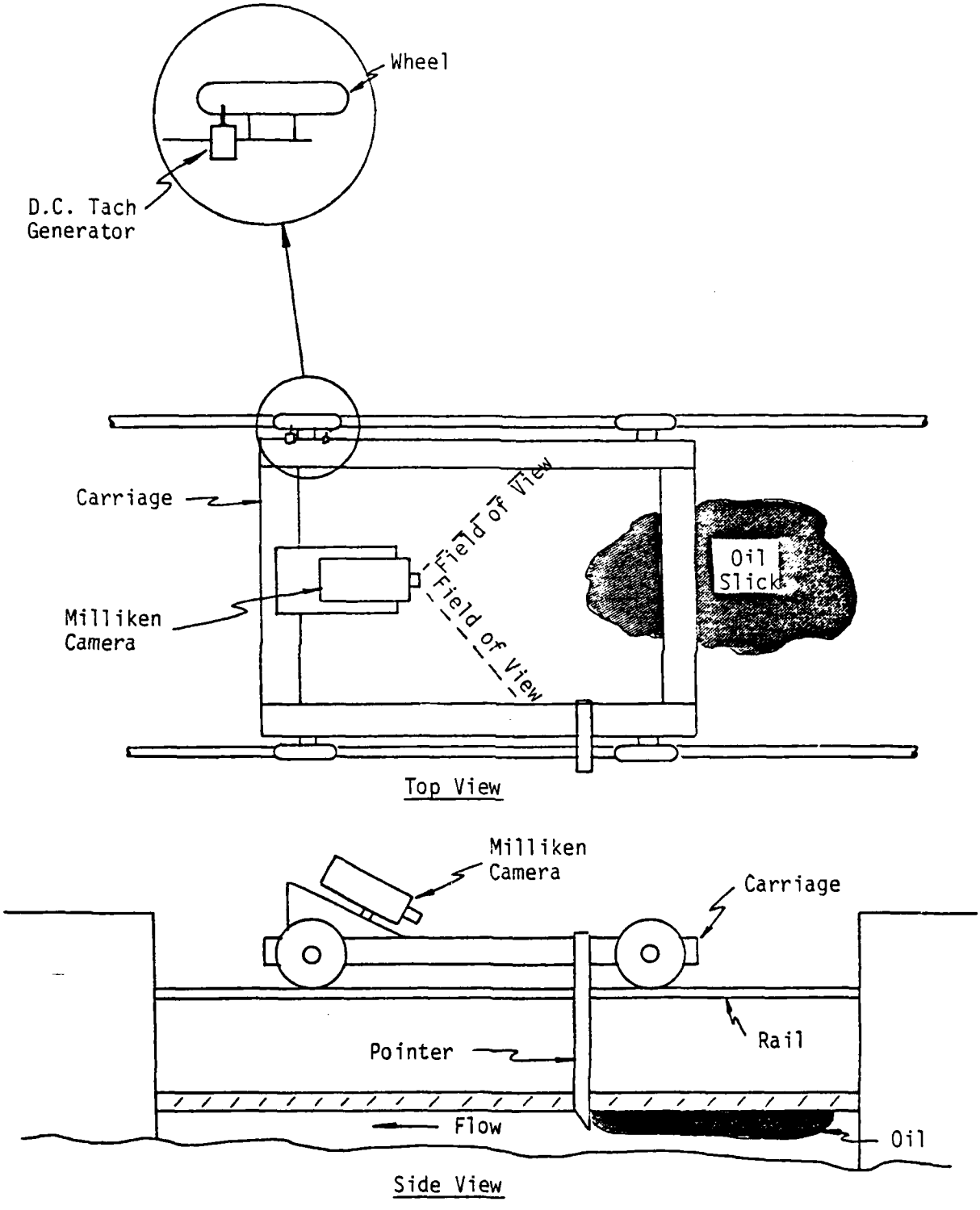

FIGURE A.2 ARCTEC ICE FLUME CARRIAGE ARRANGEMENT

A.6 Single Gap Test Apparatus

To test oil flow through a single gap, an apparatus was designed on which two ice blocks, separated by a known distance could be grown. This apparatus consisted of two 18 inch long steel boxes on which ice blocks could be grown and an upstream oil reservoir. The structure was placed in the flume and dry ice was placed inside the two steel boxes. The dry ice caused ice to be grown between the boxes. A gap of desired width was then cut using a saw. Oil was placed in the upstream reservoir, and oil flow was measured through the gap.

A.7 Surface Tensiometer

The surface tension of the oil was measured by means of a Fisher Model 20 Surface Tensiometer. The tensiometer is essentially a torsion-type balance. A platinum iridium ring of precisely known dimensions is suspended from a counter balanced level arm and immersed in the oil which is being tested. The lever arm is held horizontal by torsion applied to a taught stainless steel wire, clamped to the arm. By increasing the torsion in the wire, the lever arm is raised, also raising the ring which carries with it a film of oil. The force necessary to pull the test ring from the surface of the oil is read on the dial of the instrument. This force can then be converted to give the surface tension of the oil. This tensiometer meets ASTM specifications B-971 and D-1331.

APPENDIX B

OIL CLEANUP

After each test the oil released from the oil reservoir had to be collected and placed back in the reservoir before the next test could take place. In addition, any small amounts of oil which could not be collected had to be removed from the surface of the water and the sides of the flume.

During the single gap tests, cleanup was a relatively simple matter. A baffle was placed downstream of the single gap test apparatus, at a distance where it would not interfere with the test results. This baffle prevented oil from reaching the tail tank of the flume and possibly being sucked into the pump. After the test was completed, the gap apparatus was lifted from the flume and the baffle was slowly pushed upstream, pushing the oil in front of it. Any remaining oil which may have escaped the baffle was cleaned up with oil absorbent cloth.

The oil/broken ice tests presented a more difficult cleanup problem because the ice blocks were mixed with the oil. Again a baffle was placed far downstream in the flume. The flume pump was turned on. The ice blocks were held under water until the oil floated off them to the surface. The blocks were then pushed under the baffle and carried further downstream by the current. When all of the ice blocks were clear of the oil slick, the baffle was slowly moved back upstream to form the oil reservoir for the next test. Any significant oil remaining with the ice blocks was collected with small weir type skimmers and returned to the oil reservoir. Any remaining oil was cleaned up with oil absorbent cloth.

APPENDIX C

DERIVATION OF RELATIONSHIPS FOR OIL FLOW THROUGH A SINGLE GAP

In general, a functional relationship can be written between all of the dependent and independent variables for a given physical system. The Buckingham Pi (π) Theorem states that the number of independent dimensionless groups (π - terms) of these variables required to correlate all of the variables is equal to $n - m$, where n is the number of variables and m is the number of basic dimensions included in the variables. For the case of oil flowing through a single gap, the following variables are significant:

v_o = velocity of the oil

v_D = velocity of the driving medium

δ = thickness of the oil slick

w = width of the ice gap

g = acceleration due to gravity

μ_o = viscosity of the oil

ρ_o = density of the oil

ρ_D = density of the driving medium.

The relationship between these variables can be stated as:

$$\phi_1 \ (v_o, v_D, \delta, w, g, \mu_o, \rho_o, \rho_D) = 0 \ . \qquad (C.1)$$

Since there are eight variables and three basic dimensions of length, mass, and time, there will be five independent dimensionless terms. Non-dimensionalizing Equation (C.1) by using v_D, w, and ρ_D as the repeating variables gives the relationship between the five non-dimensional terms as:

$$\phi_2 \ \left(\frac{v_o}{v_D}, \frac{\delta}{w}, \frac{\mu_o}{v_D \ w \ \rho_o}, \frac{gb}{{v_D}^2}, \frac{\rho_o}{\rho_D}\right) = 0 \ . \qquad (C.2)$$

The third term in Equation (C.2) expresses a ratio between viscous forces and inertial forces, and therefore is a form of Reynolds Number. The fourth term in Equation (C.2) expresses a ratio between frictional forces and inertial forces, and therefore expresses a Froude Number. Equation (C.2) can be rewritten as:

$$\phi_3 \ \left(\frac{v_o}{v_D}, \frac{\delta}{w}, \frac{\rho_o}{\rho_D}, Re \ , Fr^2\right) = 0 \ . \qquad (C.3)$$

Equation (C.3) states that there exists a relationship between the five dimensionless groups listed on the left hand side of the equation. Experimental data is required to determine the exact relationship, but in general, the relationship can be stated as:

$$\frac{v_o}{v_D} = a_1 \left(\frac{\delta}{w}\right)^{a_2} \left(\frac{\rho_o}{\rho_w}\right)^{a_3} Re^{a_4} \left(Fr^2\right)^{a_5} + a_6 \ , \qquad \text{(C.4)}$$

where a_1 through a_6 are the empirical constants which must be evaluated from the experimental data.

If the oil slick thickness to gap width ratio is held constant, Equation (C.4) can be rewritten as:

$$\frac{v_o}{v_D} = a_7 \left(\frac{\rho_o}{\rho_w}\right)^{a_3} Re^{a_4} \left(Fr^2\right)^{a_5} + a_6 \qquad \text{(C.5)}$$

where

$$a_7 = a_1 \left(\frac{\delta}{w}\right)^{a_2} \ . \qquad \text{(C.6)}$$

Analysis of the results of the oil flow through a single gap experiments determined that a_3, a_4, and a_5 were independent of oil type. The values of these constants are:

$$a_3 = 1.0 \qquad \text{(C.7a)}$$

$$a_4 = 1.0 \qquad \text{(C.7b)}$$

$$a_5 = -1.0 \ . \qquad \text{(C.7c)}$$

Substituting into Equation (C.5) yields:

$$\frac{v_o}{v_D} = a_7 \left(\frac{Re}{Fr^2}\right) \left(\frac{\rho_o}{\rho_w}\right) + a_6 \ . \qquad \text{(C.8)}$$

Note that Equation (C.8) is identical to Equation (3.8) in the text, where $a_7 = K_1$ and $a_6 = K_2$.


DATE
ILME